Department of Physics and Astronomy
Heidelberg University

Bachelor Thesis in Physics
submitted by

Johannes Dreckhoff

born in Düsseldorf (Germany)

2023

Why Membrane Curvature Induces a Selection Mechanism Leading to Sharp Lipid Patterns

This Bachelor Thesis has been carried out by Johannes Dreckhoff at the
Institute of Theoretical Physics in Heidelberg
under the supervision of
Prof. Dr. Andreas Mielke

Abstract:

Nowadays lipid bilayer membranes are seen as essential for the functionality of the cell, with segregated regions of different lipid constituency for specific purposes. In recent times biochemists focused more on the connection between membrane curvature and lipid or protein concentration. S. Leibler and D. Andelman provided an effective model for the description of the concentration of the components of such membranes in 1987. R. Kaiser showed that their description was compatible with a model for fields underlying a conservation law, reproducing the patterns observed in the lipid concentrations in experiments.

We show that the results obtained above are theoretically reproducible under the addition of new terms in the Hamiltonian and how quantitative dependencies are changing when omitting such terms. We also show what mechanism dampens the growth and leads to a selection of only one growing mode in Fourier space. Not only is this necessary for the finite growth of the modes, but also explains why observed patterns in e.g. cell-membrane lipid concentrations appear sharp in experiment. This serves as the basis for further analysis, as one only has to consider one non-vanishing mode in such systems in at least some approximation.

Kurzfassung:

Doppellipidschichten werden heutzutage als essentiell für die Funktionalität der Zelle angesehen, mit Regionen unterschiedlicher Lipidzusammensetzung für unterschiedliche Aufgaben. Insbesondere der Zusammenhang zwischen der Membrankrümmung und der Lipid- oder Proteinkonzentration ist seit einiger Zeit ins Interesse von Biochemikern gerückt. Schon 1987 haben S. Leibler und D. Andelman ein effektives Modell zur Beschreibung der Komponenten solcher Membranen vorgestellt. R. Kaiser zeigte nun, dass diese Beschreibung kompatibel mit einem Modell für Felder, welche einem Erhaltungssatz unterliegen, ist, und dabei die experimentell beobachteten Muster in Lipidkonzentrationen reproduziert.

Wir zeigen die theoretische Reproduzierbarkeit obiger Ergebnisse unter der Hinzunahme neuer Terme im Hamiltonian und wie sich quantitative Abhängigkeiten durch diese ändern. Ebenso zeigen wir, welcher Mechanismus für das endliche Wachstum einer und das Verschwinden aller anderen Moden im Fourierraum sorgt. Dies erklärt auch, warum experimentell beobachtete Muster in Lipidkonzentrationen in Zellmembranen scharf erscheinen, obwohl es möglicherweise mehrere initial wachsende Moden geben kann. Unsere Ergebnisse dienen auch als Grundlage für weitergehende Untersuchungen, da man, zumindest in gewisser Näherung, nur eine nichtverschwindende Mode im nichtlinearen Regime beachten muss.

Contents

The sources for all figures used can be found in the list of figures at the end of this thesis. If no source is credited the figure is self-made.

Chapter 1

Introduction

(a) Patterns are found everywhere throughout nature. For animals, they are often essential as a form of camouflage, as seen by the pattern the fur of this Malayan tiger shows.

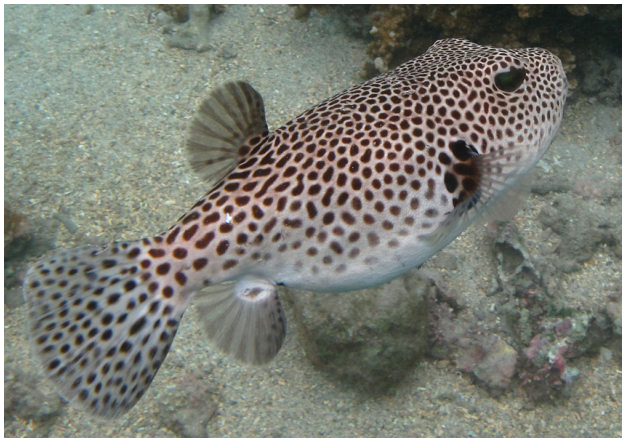

(b) This picture of the naturally occurring pattern on a pufferfish (Arothron stellatus) is an example of a Turing pattern appearing in nature.

Figure 1.1: Examples of patterns appearing in nature.

1.1 Motivation

Whenever we look around us, a striking fact about our world is that it is comprised of myriads of vastly different forms of matter. And while the physical description of such systems is often surprisingly reduced, the macroscopic world that emerges is filled with interesting phenomena. Why does a tiger develop a pattern like in 1.1a, when there is no trace of such a pattern in its microscopical constituents?

While the task of many aspects of physical research is to explain how everything is built up, pattern formation asks why simple microscopical building blocks lead to interesting macroscopic

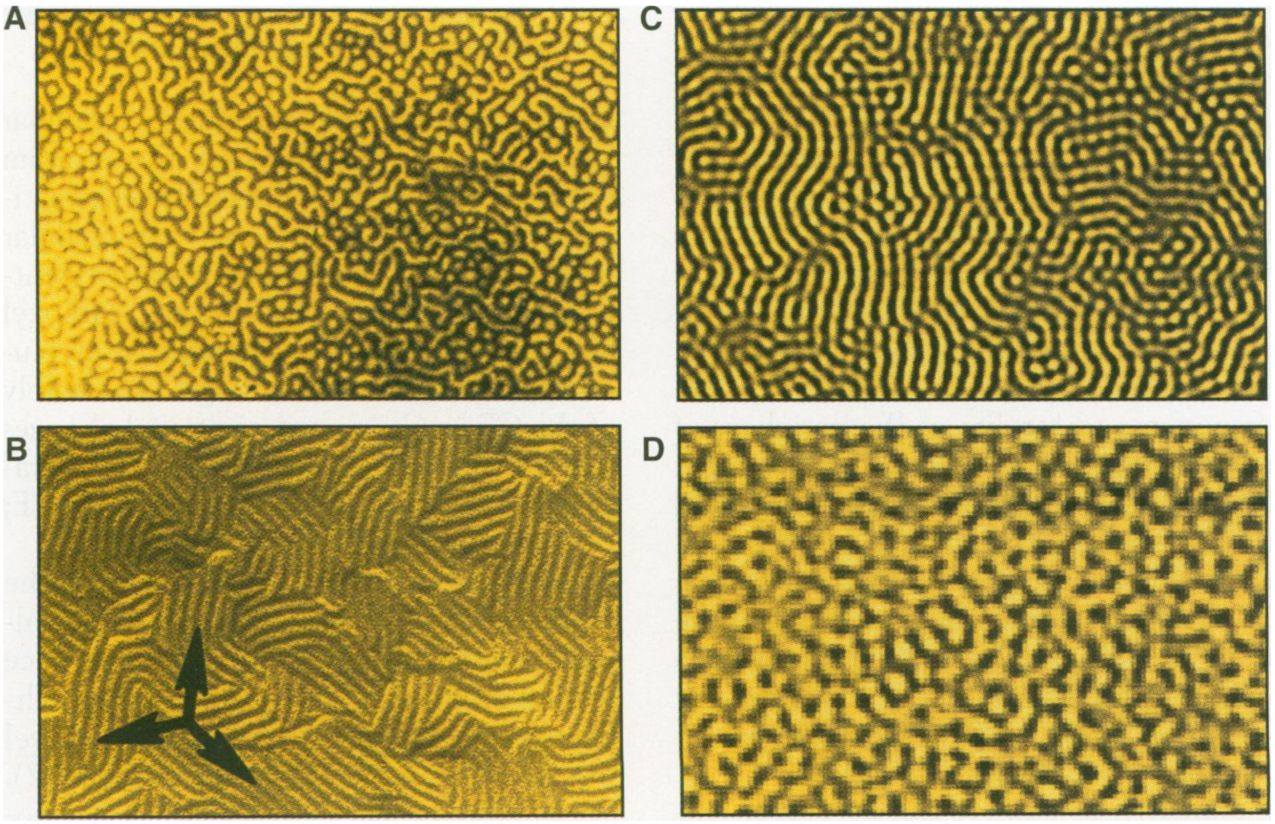

Figure 1.2: Patterns appear in vastly different physical systems. Seen here are (A) alternating superconducting and normal regions in a type I superconductor, (B) a "ripple" phase in a biological vesicle, (C) a Turing pattern in a chemical reaction-diffusion system and (D) fluctuations in a CO2 gas preceding the formation of a convective roll pattern under a Rayleigh-Benard instability.

systems. One of the first pioneers of pattern formation was Alan M. Turing. In his paper [Tur52] he laid down the foundational idea that in nature, the natural state of a system will often not be the homogeneous one, but instead a wide variety of patterns may appear even in the simplest systems. Turing described that a homogeneous or random mixture of two fluids may generate spatially periodic patterns, so called "Turing patterns", as seen on the skin of the pufferfish in Fig. 1.1b.

What Turing and others have developed has turned into a wide variety of approaches and applications of the research on and uses of pattern formation, including (but not limited to) fluid dynamics, crystal growth, ecology [Mai04] or even in the description of brain activity [Ple+21].

An important feature of such patterns (as is often the case with emergent phenomena) is the independence of the emerging pattern from the physical system [SA95]. As can be seen in Fig. 1.2, stripe patterns appear in vastly different physical systems, ranging from superconductors to biological cells, chemical reactions and gases.

A key ingredient is that we are dealing with non-equilibrium systems, which means the equations of motion are often non-linear. A fundamental task is therefore to explain what parts of a system (one often talks of "modes" when dealing with problems in Fourier-space) will grow to different (macroscopic) scales than the rest of the system.
An interesting field of study is the research on biological membranes. Despite their importance, biochemists had cast them aside for a long time, as the research-conditions were quite cumbersome. But in recent times new insights were gained. It turns out "membranes are more mosaic than fluid" [Eng05], referring to their patchy nature as they are most often comprised of different constituents, e.g. different lipids and proteins. These proteins are described as floating in a "sea", the lipid bilayer. The interactions between lipid composition, local protein concentration and the spontaneous curvature of the lipid bilayer membrane were found to be quiet complex [HR18], too complex to explain in a short overview. For example, certain proteins favour regions with certain lipid composition, which in return favour certain membrane curvatures.
In that light, MacMahon and Gallop [MG05] described that the membrane curvature should then no longer be understood as a simple consequence of the cell activity and its surroundings, but rather as an active means to create domains of the membrane with different constitution. They emphasised the interplay between the membrane curvature and the local composition, especially with regards to "curvature-sensing" proteins. Thus, what at first appeared to be only of secondary interest is in fact an essential component in the understanding of cells.
In a simplified case, one may only ask about the composition of a lipid bilayer of two different lipids, as this is the basis to incorporate proteins later on. Similar to what [Eng05] described, the composition of the cell membrane is not homogeneous, but instead displays a pattern. And this pattern is strongly influenced by the curvature of the cell, as suggested by [MG05]. In the thesis [Kai22] the spatio-temporal pattern formation was investigated with the result of developing an effective model only for the local composition.
In leading order in momenta, this model predicts the onset of pattern formation and the typical wavelength of a pattern, yet it lacks a mechanism of limiting their growth. From looking at Figure 1.3 one may already suspect that the sharpness of the pattern has to be linked with a mechanism that dampens all but one mode in momentum space.
The aim of this thesis is therefore to look at the robustness of the developed effective model from [Kai22] under the addition of new terms in the Hamiltonian and to explain what mechanism leads to a finite growth of modes and to sharp resulting patterns.

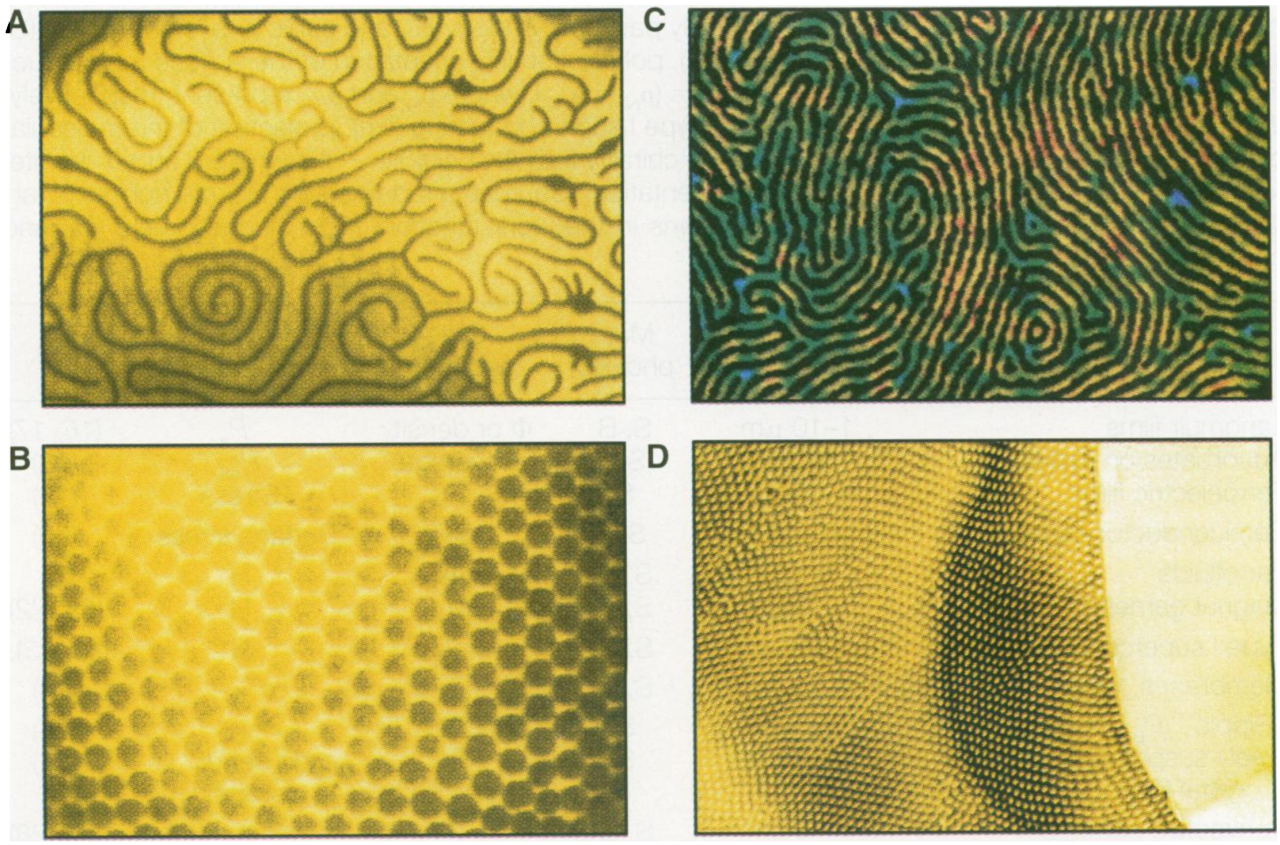

Figure 1.3: Displayed are the formations of stripe and bubble patterns forming in organic 2D and 3D systems. (A) and (B) depict a Langmuir film at an air water interface, displaying (A) a stripe and (B) a bubble (or hexagonal) pattern. (C) and (D) show a film of block copolymers exhibiting the same formations of stripe and bubble patterns.

1.2 Structure of the Thesis

The first section after the introduction will provide the reader with some needed background information. We will talk about concepts in pattern formation and lipid bilayers in general. After that we will introduce the concentration of two lipid species which will form patterns. We then explain the differences in the behaviour of the possible patterns and how to implement the description of such patterns into a Hamiltonian. This Hamiltonian-formulation introduces the coupling to the membrane curvature. After having introduced the membrane curvature we explain how to calculate an effective Hamiltonian that averages over the curvature and how to calculate rates of growth for different field modes.
In the following section we explain how the results of [Kai22; LA87] change if one introduces a new term to the Hamiltonian. We explain the necessity to introduce higher order terms into the Hamiltonian and show that they recover the qualitative results found previously. We thereby show that, at least for qualitative research, it is not necessary to include such terms in the

Hamiltonian.
The next section builds up on the results found by [Kai22]. We explain the need for a mechanism that leads to a finite growth of the field modes. We show that this mechanism is provided by higher-than-quadratic-order mode-coupling. This mechanism also leads to a selection of growing modes, thereby sharpening the emerging pattern.
The last section is a summary of all things found and an outlook on what is left to do. The appendix is located after the outlook and includes many calculations that are necessary but lengthy and not of core importance. The thesis ends with a list of figures including the sources for all images, a list of tables and the bibliography.

Chapter 2

Physical Background

2.1 Pattern Formation

Pattern formation is a specific area in the field of self organisation, which deals with complex systems, their instabilities and symmetry breakings [Wal12]. An important example is the laser, which may be described as a self organised phenomenon [Hak77]. Since the discussed systems may become very complex, the analysis under the aspect of self organisation can become arbitrarily complicated.

As the name suggests, pattern formation focuses (mostly) on the appearance of visible patterns in media, e.g. the patterns visible in Fig. 1.2 and 1.3. The exact process in which one can analyse a system will vary depending on the subject and we cannot give a general introduction, but we can briefly explain the concepts needed for this thesis.

In some cases, like the one we are interested in, one may look at a system's degrees of freedom, e.g. a single one named ϕ, and its time evolution $\partial_t \phi = F(\phi, \boldsymbol{X})$, where $\boldsymbol{X}$ describes an array of exterior parameters (e.g. the temperature or the bending rigidity modulus of a membrane). One is often interested in the emergence of patterns from homogeneous initial states, usually described by $\phi = 0$. Therefore one assumes a set of parameters $\boldsymbol{X}_0$ with which the solution $\phi = 0$ is stable (in the sense that linear excitations from the homogeneous state decrease asymptotically to zero, as described in A.8).

When transferring this to Fourier-space and assuming small momenta, one can usually extract a linear rate of growth σ_k (c.f. A.3 for a detailed example for our case):

$$\partial_t \phi_k = \sigma_k(\boldsymbol{X})\phi_k + \mathcal{O}(\phi^2) \tag{2.1.1}$$

which is also a function of the exterior parameters $\boldsymbol{X}$, and the stability of the homogeneous solution usually leads to all rates of growth being negative, $\sigma_k(\boldsymbol{X}_0) < 0 \ \forall k$. By varying the

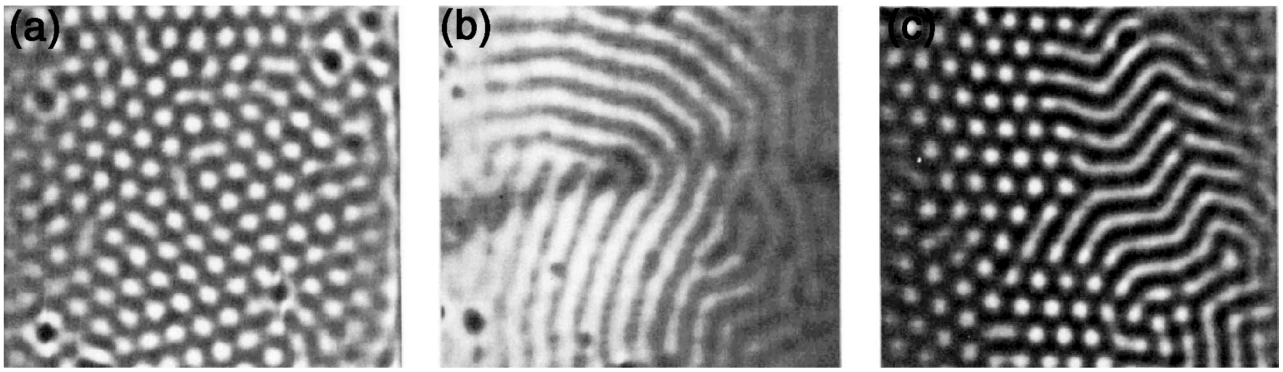

Figure 2.1: Depicted are hexagon and stripe patterns in chlorite-iodide-malonic-acid (CIMA). In (a) a hexagonal pattern is shown. Figure (b) shows a stripe pattern and (c) depicts the boundary between hexagons and stripes. All images where taken at the same value of the control parameter (in this case the acid concentration).

parameters, one may achieve that a set of modes gains a positive rate of growth. In the simplest case, only one mode ϕ_k has a positve rate of growth. In position space in e.g. one dimension, this then leads to the emergence of a stripe pattern with wavelength $\lambda = \frac{2\pi}{k}$, coining the term pattern formation [CH93]. In more dimensions, this can quickly lead to interesting patterns. Only three growing modes are necessary to form hexagonal patterns in two dimensions [CG09], as can be seen in Fig. 2.1.

2.2 Lipid Bilayers

In this thesis we shall only be concerned with mixed lipid bilayers.They are not only the starting point to implement more specific effects and are a model system for understanding biological membranes, see [PS95], they are also a crucial component in the biological organism, where even small changes in lipid composition can have major effects on biological functions [HR18]. A bilayer is a membrane structure formed by amphiphilic (both hydrophobic and hydrophilic) molecules in a solvent, often water [Ran81]. The amphiphilic nature of the constituents brings the molecules to point their hydrophilic heads towards the solvent and their hydrophobic tails towards one other [SR21], creating the bilayer structure, as can be seen in Fig. 2.2. Related to such bilayers are monolayers, often found at the boundary of two immiscible solvents, as the hydrophobic and -philic parts again have favoured directions of orientation [LA87]. But for the effects discussed here, a distinction of the two is not necessary, as only the feature that both can build up curvature is important.

When using a simple description for the lipids in a bilayer, we can assume them to have conical shape. Either the hydrophilic heads, pointing "outward" have a larger diameter or the hydrophobic tails, pointing "inward". As can be seen from Fig. 2.2 this leads to a spontaneous

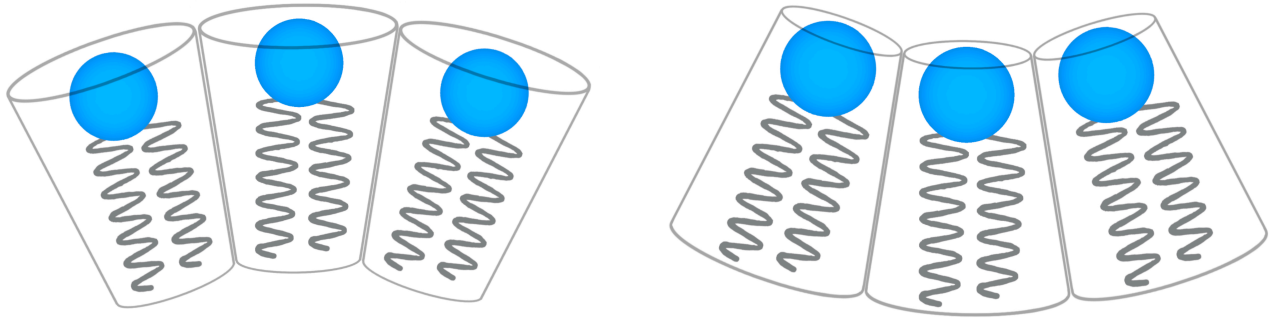

(a) An example for lipid-geometry leading to positive curvature.

(b) An example for lipid-geometry leading to negative curvature.

Figure 2.2: The geometry of different lipids can lead to the development of membrane-curvature, see [AK07].

curvature of the cell. This means, when more lipids of a certain type A are present locally than of type B, the local curvature will favour the curvature associated to the lipids of type A. If one defines ϕ as a measure of concentrations, e.g. $\phi = 1$ means only type A is present and $\phi = 0$ means only type B is present, then, as explained above, the curvature is coupled to the lipid composition ϕ.

The idea of many ([Hel73; Räd+95; SJW84; Cam+14] to only name a few) was to address this phenomenon by introducing a local description of the composition ϕ and of the local curvature, paired with a coupling of both.[1]

While the above mentioned authors tried various different implementations of the curvature, we will focus on the ansatz of Leibler & Andelman [LA87].

2.3 Concentration as a Degree of Freedom

In general, ϕ is just a generic internal DOF which can be described by a continuous field. The Hamiltonian (2.5.4) we use later only uses a small gradient approximation, independent of what ϕ "is".

The interesting assumption [Kai22] did was to assume that if ϕ describes the concentration of

[1] This type of model is more general than we will discuss. In general ϕ can be thought of as a generic **internal** degree of freedom of the lipid layer, leading to an "internal phase transition", see [Nag80] and [GGS77]. Instead of the concentration of two lipid species we use in this thesis, one could also look at the local area per amphiphile, as Leibler & Andelman suggested. The important feature discussed here is that the internal DOF are coupled to the external DOF of the membrane, in the simplest case its local curvature, thereby inducing "curvature instabilities" as L.&A. termed them. Only the fact that we assume a continuity equation to hold for ϕ restricts the results.

two lipids, it has to obey a continuity equation of the form

$$\partial_t \phi = -\nabla j \tag{2.3.1}$$

where j is the associated particle flux. With the further assumption that the particle flux is proportional to the negative gradient of the chemical potential (as the conjugate variable to the density)

$$j = -M \nabla \mu \tag{2.3.2}$$

where the proportionality constant M is called the "mobility", and that $\mu = \frac{\delta \mathtt{H}}{\delta \phi}$, one obtains the time evolution of the field ϕ as

$$\partial_t \phi = M \Delta \left(\frac{\delta \mathtt{H}}{\delta \phi} \right) \tag{2.3.3}$$

which is not necessarily true for a generic degree of freedom ϕ.

2.4 Pattern Formation and Demixing

The assumption from 2.3 that [Kai22] took was necessary to investigate if cell membranes, which have been shown to display pattern-forming behaviour, could be described by a model of two demixing fluids, i.e. we would naively expect *demixing* instead of *pattern forming*. We need to briefly explain what we mean by both terms.

The systems we investigate may show two different behaviours of patterns arising from a homogeneous state, which are characterised by their **critical wave vector** q_c. This is defined as the wave vector for which the rate of growth $\sigma(q)$ first becomes positive when varying the critical parameter of the system.[2] In a first approximation, we assume our system to be in a region of small critical parameter. Then q_c predicts the length scale $\lambda = 2\pi/q_c$ of the growing perturbation [CG09].

The first type we call "true pattern forming systems", as these develop patterns of finite wavelength. Such systems have a **non-zero critical wave vector** q_c. The simplest example of such a system is described by the Swift-Hohenberg model [CG09], for which the equation for the rate of growth $\sigma(q)$ for the q mode in Fourier space is

$$\sigma(q) = \varepsilon - \left(q^2 - q_c^2\right)^2 \tag{2.4.1}$$

with ε being the critical parameter and q_c being the critical wave vector, as seen in Fig. 2.3a.

[2] One usually scales the critical parameter s.t. it is zero when the first positive rates of growth appear.

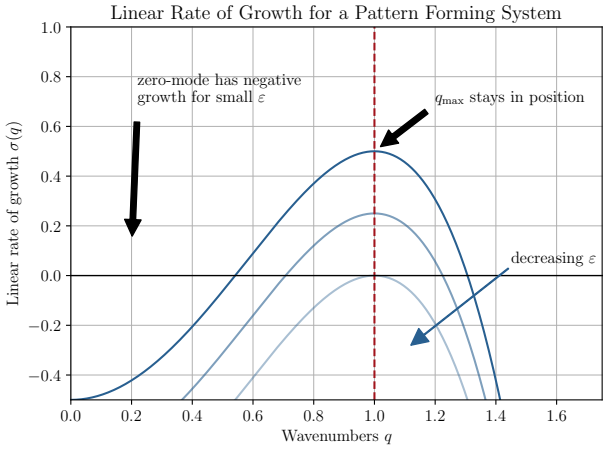

(a) The typical behaviour of the linear rate of growth of the q mode for a pattern forming system. The range of wavelengths with positive growth is finite and excludes zero. The position of the wave vector of maximum growth does not vary with the critical parameter ε, thereby the critical wave vector is non-vanishing. The function used was (2.4.1) with varying values of ε and $q_c = 1$.

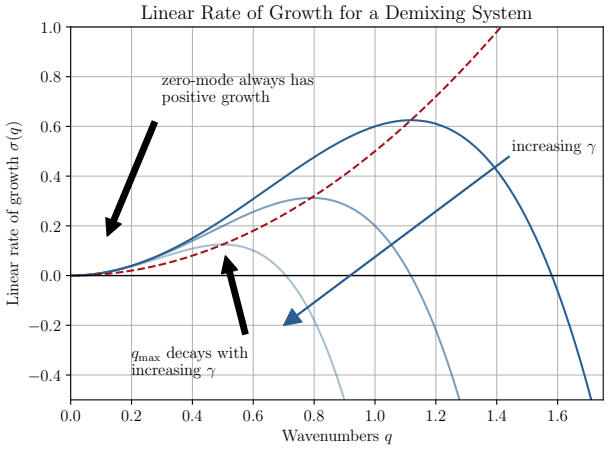

(b) The typical behaviour of the linear rate of growth of the q mode for a demixing system. The range of growing modes includes the 0-mode. Decreasing $1/\gamma$ shifts the wave vector of maximum growth towards zero, therefore the system has vanishing critical wave vector. The graph depicted here was plotted using (2.4.3) with $D = 1$ and different values of γ.

Figure 2.3: Here depicted are the graphs for the rates of growth $\sigma(q)$ for the Swift-Hohenberg and the Cahn-Hilliard model, leading either to pattern forming or demixing behaviour. The dashed lines indicate the changes in the wave vector of maximum growth. The intersection of said lines with the x-axis indicates the critical wave vector.

Since q_c is a direct parameter of the model, one immediately sees that the critical wave vector is non-vanishing for $q_c \neq 0$. In such systems, for small critical parameter, the wave vector of maximum growth is always near the critical wave vector, and therefore predicts a pattern of finite wavelength.

Since the characteristic factor of such systems is that the first modes to have positive growth are away from the zero-mode, i.e. the area of positive growth emerges away from zero, we can characterise a system as a pattern forming system if the zero mode is not included in the finite area of positive growth for small critical parameters:

$$\sigma_{\text{p.f.}}(k) > 0 \Leftrightarrow k \in [k_{\min}, k_{\max}] \not\ni 0 \tag{2.4.2}$$

We call the alternative behaviour "demixing" as this behaviour resembles two immiscible fluids, like water and oil, demixing and forming large patches of homogeneous constituency. The important feature is that such systems have **vanishing critical wave vector** q_c, i.e. the first modes to have positive growth when increasing the critical parameter are arbitrarily close to

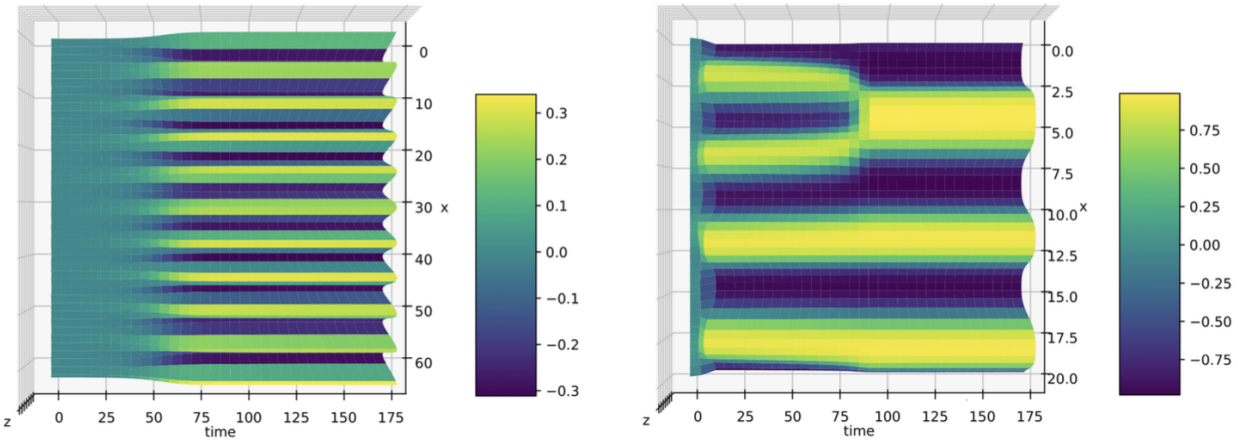

Figure 2.4: The evolution of a concentration field ϕ, as indicated by the colour, can be seen for two different cases. On the left a typical pattern forming process can be seen, as described by the Swift-Hohenberg model. From a homogeneous ground state a pattern emerges which is stable in time. On the right, a typical demixing process can be seen, usually described by the Cahn-Hilliard model. An apparently stable pattern reduces to one of larger wavelength by two stripes merging.

$q = 0$. The simplest example of such a system is given by the Cahn-Hilliard model [CG09; Kai22] for which the rate of growth $\sigma(q)$ is given by

$$\sigma(q) = Dq^2\left(1 - \gamma q^2\right) \tag{2.4.3}$$

as seen in Fig. 2.3b. Indeed, such systems often describe two fields (e.g. liquids) obeying a continuity equation. Therefore D is often associated with a diffusion constant. $1/\gamma$ is the critical parameter of the system.

When assuming such systems to be in a region of small critical parameter, one cannot give a prediction of a finite length scale for the growing perturbation, as $\lambda \to \infty$ for ever smaller values of the critical parameter. One rather deduces that such systems tend to form large homogeneous regions [CG09].

For both cases example behaviours are depicted in Fig. 2.4. In the case of demixing, one can see a (what seems to be stable) pattern merging together to form a new pattern with larger wavelength, resembling the tendency to form patterns with an ever increasing wavelength.

2.5 Helfrich Hamiltonian and the Ginzburg-Landau Expansion

A first problem in coupling the internal degree of freedom to the membrane shape is that a vesicle enclosed by a membrane can have all forms of shapes. The local nature of our description lies in the assumption that we may describe the form of the membrane by a height function or curvature profile $l(x, y)$ of the 2d coordinates x and y, i.e. the membrane is approximately

planar for small regions. This also assumes that the membrane does not topple onto itself.
The first to provide formulae for implementing the effect of the curvature of the membrane on the energy were Canham [Can70] in 1970 and Helfrich [Hel73] in 1973. Both, without going into detail, proposed that the bending energy was proportional to the square of the inverse bending radius, but differed in how to implement the bending modulus in different directions[3].
Orientating on Helfrichs notation, with σ being the surface tension and κ the rigidity modulus suggests[4] [Hel85]

$$\mathtt{H}_{\text{bending}} \approx \int \mathrm{d}^2x \left(\frac{\sigma}{2} \left(\nabla l\right)^2 + \frac{\kappa}{2} \left(\nabla^2 l\right)^2 \right) \tag{2.5.1}$$

One may then introduce an internal degree of freedom, described by a continuous variable $\phi(x, y)$[5]. As stated above, this ϕ can in general be any internal DOF, but we will restrict it to the case of 2.3, that is its time evolution is given by a continuity-equation.
The generic Ginzburg-Landau expansion of the Hamiltonian in terms of gradients of ϕ then suggests

$$\begin{aligned} \mathtt{H}_{\phi} = &\int \mathrm{d}^2x \left(\frac{\beta}{2} \left(\nabla \phi\right)^2 + \frac{A}{2} \left(\nabla^2 \phi\right)^2 \right) \\ &+ \int \mathrm{d}^2x \left(\frac{a_2}{2}\phi^2 + \frac{a_4}{4}\phi^4 - \mu\phi \right) \end{aligned} \tag{2.5.2}$$

This is the standard Ginzburg-Landau expansion for a field ϕ. The lower term is responsible for the phase transition. In the usual interpretation, $a_2 \sim \frac{T - T_c}{T_c}$ is proportional to the temperature above the critical one, thereby leading to the phase transition. a_4 stabilises this behaviour. We will later see that a_4 is also responsible for limiting the growth of our patterns. μ is the chemical potential.
For the coupling, one assumes a $\mathbb{Z}_2$ symmetry (i.e. we only have even powers of gradients when terms contain even powers of fields). Only considering linear terms in both l and ϕ leaves us with

$$\mathtt{H}_{\text{int}} = \int \mathrm{d}^2x \left(\Lambda\phi \left(\nabla^2 l\right) + \lambda\phi \left(\nabla^4 l\right) \right) \tag{2.5.3}$$

Plugging everything together leaves us with the Leibler & Andelman Hamiltonian for the de-

[3] More on their connection, their differences and why both ways often are equivalent can be found in [Des] in chapter 4 about Helfrich theory.

[4] This is a small gradient expansion of the full Helfrich term. As we see later, we could have started by constructing a general Hamiltonian as a gradient expansion and then identify the terms with the Helfrich terms.

[5] This variable will lead to a critical point at $\phi_0 = 0$, so it is already "normalised" to its critical value being zero.

scription of curvature induced instabilities in an internal DOF ϕ of a membrane surface:

$$\boxed{\mathtt{H}_{\mathrm{LA}} = \int \mathrm{d}^d x \left(\frac{\sigma}{2} \left(\nabla l\right)^2 + \frac{\kappa}{2} \left(\nabla^2 l\right)^2 + \frac{\beta}{2} \left(\nabla \phi\right)^2 + \frac{A}{2} \left(\nabla^2 \phi\right)^2 + \Lambda\phi \left(\nabla^2 l\right) + \lambda\phi \left(\nabla^4 l\right) + f(\phi) \right)} \tag{2.5.4}$$

In comparison to the Hamiltonian used in [LA87] we renamed b with β, not to be confused with the inverse temperature, which will not appear here. The function $f(\phi) = \frac{a_2}{2}\phi^2 + \frac{a_4}{4}\phi^4 - \mu\phi$ is important, but is seldom needed when calculating the effective Hamiltonian, since it only contains pure ϕ terms. We will therefore often use $\mathtt{H} = H + \int \mathrm{d}^d x\, f(\phi)$.

2.6 Calculating an Effective Hamiltonian

Leibler & Andelman showed that one may reduce the full Hamiltonian (2.5.4) to an effective one, to gain insight about the system [LA87]. The calculation averages over the curvature profile l. To do so, we first need to convert (2.5.4) into momentum space. For this we will use the conventions stated in A.1. To keep things tidy, we will also use some formulae from A.2. To give an overview of what we are doing (also later on), we tried to be quiet explicit here. In momentum space we therefore read

$$\begin{aligned} H &= \sum_k \left(l_k l_k^* \left[\frac{\sigma}{2}k^2 + \frac{\kappa}{2}k^4\right] + (\phi_k l_k^* + l_k \phi_k^*) \left[\frac{\lambda}{2}k^4 - \frac{\Lambda}{2}k^2\right] + \phi_k \phi_k^* \left[\frac{\beta}{2}k^2 + \frac{A}{2}k^4\right] \right) \\ &= \sum_k \left(a l_k l_k^* + b(l_k \phi_k^* + \phi_k l_k^*) + c \phi_k \phi_k^* \right) \\ &= \sum_k \left[\left(\sqrt{a} l_k + \frac{b}{\sqrt{a}} \phi_k \right) \cdot \left(\sqrt{a} l_k + \frac{b}{\sqrt{a}} \phi_k \right)^* + \left(c - \frac{b^2}{a} \right) \phi_k \phi_k^* \right] \end{aligned} \tag{2.6.1}$$

with $a = (\sigma k^2 + \kappa k^4)/2$, $b = (\lambda k^4 - \Lambda k^2)/2$ and $c = (\beta k^2 + A k^4)/2$. The red minus sign is different from the sign in [LA87] which is wrong[6]. Now the construction of the effective Hamiltonian is easy. One substitutes correctly, performs the Gaussian integration over $\tilde{l}_k := \sqrt{a} l_k + \frac{b}{\sqrt{a}}\phi_k$ and gets (up to an irrelevant normalisation factor)

$$H_{\mathrm{eff}} = \sum_k \left(c - \frac{b^2}{a} \right) \phi_k \phi_k^* \tag{2.6.2}$$

[6] As Leibler and Andelman set the term which is changed by this sign to zero, it does not matter for the results they obtain.

Since we only consider an expansion up to fourth order, we expand b^2/a using (A.4.2)

$$\frac{b^2}{a} = \frac{\Lambda^2}{2\sigma}\frac{\left(k^2 - k^4\frac{\lambda}{\Lambda}\right)^2}{k^2 + k^4\frac{\kappa}{\sigma}} = \frac{\Lambda^2}{2\sigma}\left(k^2 + k^4\left(-2\frac{\lambda}{\Lambda} - \frac{\kappa}{\sigma}\right)\right) + \mathcal{O}(k^6) \tag{2.6.3}$$

to arrive at

$$H_{\text{eff}} = \sum_k \left\{\frac{q^2}{2}\left(\beta - \frac{\Lambda^2}{\sigma}\right) + \frac{q^4}{2}\left(A + \kappa\frac{\Lambda^2}{\sigma^2} + 2\lambda\frac{\Lambda}{\sigma}\right)\right\}\phi_k\phi_k^* \tag{2.6.4}$$

as the effective Hamiltonian in momentum space. When transforming this back to position space using (A.2.2), using the same conventions as above, we arrive at (now including the $f(\phi)$ term)

$$\boxed{\mathtt{H}_{\text{eff}} \approx \int \mathrm{d}^d x \left[\frac{B}{2}\left(\nabla\phi\right)^2 + \frac{C}{2}\left(\nabla^2\phi\right)^2 + \frac{a_2}{2}\phi^2 + \frac{a_4}{2}\phi^4 - \mu\phi\right]}$$
$$\text{with} \qquad B = \beta - \frac{\Lambda^2}{\sigma} \quad C = A + \kappa\frac{\Lambda^2}{\sigma^2} + 2\lambda\frac{\Lambda}{\sigma} \tag{2.6.5}$$

which is the Hamiltonian used in [Kai22].

2.7 Computing the Linear Rates of Growth

From (2.6.5) one may now compute the linear rate of growth, following A.3. The linear rate of growth σ_k is the rate at which the k-mode will grow in the regime of small ϕ_k, i.e. $\phi \sim \phi_{k,0} \cdot \exp\left(i\boldsymbol{k}\boldsymbol{x} + \sigma_k t\right)$. The linear part of H_{eff} is given by $\mathcal{L}(\nabla^2) = (a_2 - B\nabla^2 + C\nabla^4)$.[7] This leads, following the definition $\sigma_k = \frac{-k^2 M}{2}\mathcal{L}(-k^2)$ from (A.3.13), to the linear rate of growth found by [Kai22]

$$\boxed{\sigma_k = -a_2 k^2 - Bk^4 - Ck^6}$$
$$\text{with } B = \beta - \frac{\Lambda^2}{\sigma} \quad C = \kappa\frac{\Lambda^2}{\sigma^2} \tag{2.7.1}$$

where [Kai22] set $M = 1, A = \lambda = 0$ (in accordance with Leibler & Andelman) and ignored the $\Delta\mu$ term (as described in the appendix) in the time evolution, leading to a missing factor of $1/2$. Per definition $a_2 > 0$ and $C > 0$. Then B may change its sign if $\Lambda \geq \Lambda_c = \sqrt{\beta\sigma}$. For larger and larger values of Λ, σ_k will eventually start at $\sigma_k(k = 0) = 0$, then decrease with increasing k, increase for intermediate k and then finally decrease again for large k. The two possible cases for the behaviour of $\sigma(q)$ with negative B can be seen in Fig. 2.5. The system has a finite

[7] Linear means the Hamiltonian can be written as $H = \int \mathrm{d}\phi\ \phi\frac{\mathcal{L}}{2}\phi + \mathcal{N}$ where $\mathcal{N}$ is the part of the Hamiltonian of higher than quadratic order.

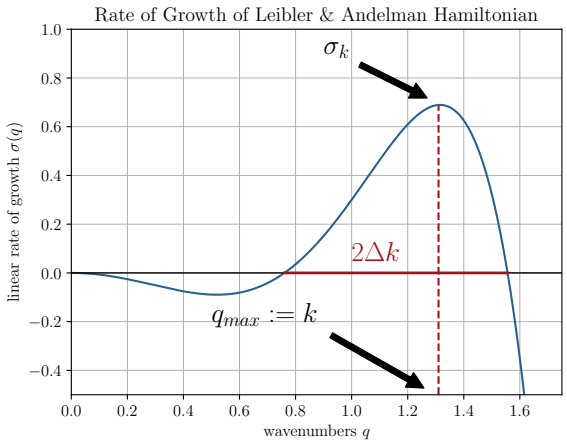

(a) The rate of growth from (2.7.1) for exemplary values of $a_2 = 0.7$, $B = -1.5$ and $C = 0.5$. This rate of growth is only positive in a finite region excluding zero, thereby showing the behaviour we expect for pattern forming systems. We marked σ_k as the largest rate of growth together with its index k and the area of positive growth $2\Delta k$ for evaluating the error of approximation done in A.7.

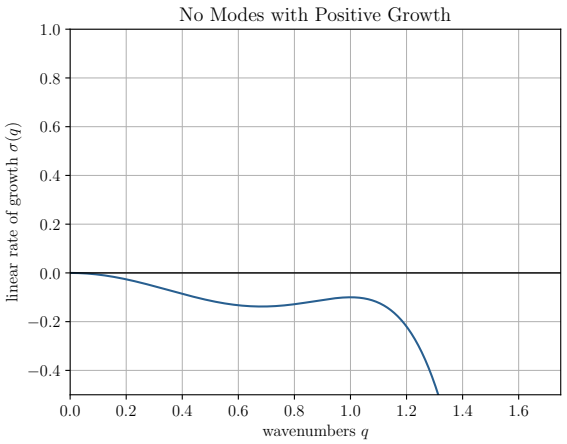

(b) Again the rate of growth from (2.7.1) with the same values, but with a slightly lower $B = -1.1$. In this case, no modes with positive rate of growth are present in the system.

Figure 2.5: The effective Leibler & Andelman Hamiltonian (2.5.4) may show different behaviours for the rate of growth $\sigma(q)$. This signals a bifurcation of the system, where by a variation of a parameter (in this case B) the system's behaviour may drastically change.

regime $[k_{\min}, k_{\max}]$ excluding zero containing modes with positive linear rate of growth $\sigma_k > 0$. The critical wave vector q_c as found by [Kai22] is given by

$$q_c = \sqrt{\frac{\sigma\Lambda^2 - \sigma^2\beta}{2\Lambda^2\kappa}} \tag{2.7.2}$$

and is non-vanishing for $\Lambda^2 > \sigma\beta$, thereby leading to the system showing pattern formation, see 2.4.

Chapter 3

Probing the Robustness of the Model

3.1 Addition of new Hamiltonian Term

The first question we want to answer is: "How robust are the results obtained from [Kai22] under the addition of new terms to the Hamiltonian (2.5.4)?" The term we introduce is the simplest possible, a term coupling directly to the absolute height l with respect to a reference height l_0, which we choose itself to be zero. This results in an additional term

$$H_{\text{add.}} = \int \mathrm{d}^d x \, \frac{\gamma}{2} l^2 \tag{3.1.1}$$

This term penalises deviations of l from the reference height $l_0 = 0$. This could e.g. be interpreted as a near-planar approximation of the membrane, as one could define a reference height l_0 in this case. In light of this interpretation, one can expect that deviative effects will only appear in higher orders, as they are suppressed in the lower orders since our approximation is near-planar. Since we integrate out the field l, only average effects of l will be visible in the end result. Previously this was through σ and κ appearing in our effective constants B and C, since σ and κ were the constants penalising the curvature of l. By introducing γ, which penalises every deviation from l_0, we can expect that γ will replace some of the dependencies from σ and κ. We will confirm these suspicions later on.
The calculation of the new $\mathtt{H}'_{\text{eff}}$ is very similar to the one leading to (2.5.4). Since in momentum space

$$H_{\text{add.}} = \sum_k \frac{\gamma}{2} l_k l_k^* \tag{3.1.2}$$

we have

$$\begin{aligned} H' &= \sum_k \left\{ l_k k_l^* \left(\frac{\gamma}{2} + k^2 \frac{\sigma}{2} + k^4 \frac{\kappa}{2} \right) + (\phi_k l_k^* + l_k \phi_k^*) \left(k^4 \frac{\lambda}{2} - k^2 \frac{\Lambda}{2} \right) + \phi_k \phi_k^* \left(k^2 \frac{\beta}{2} + k^4 \frac{A}{2} \right) \right\} \\ &= \sum_k \left(\sqrt{a} l_k + \frac{b}{\sqrt{a}} \phi_k \right) \cdot \left(\sqrt{a} l_k + \frac{b}{\sqrt{a}} \phi_k \right)^* + \left(c - \frac{b^2}{a} \right) \phi_k \phi_k^* \end{aligned} \tag{3.1.3}$$

with $a = (\gamma + \sigma k^2 + \kappa k^4)/2$, $b = (\lambda k^4 - \Lambda k^2)/2$ and $c = (\beta k^2 + A k^4)/2$.
Again, to calculate the effective Hamiltonian in leading (i.e. fourth) order, we need to expand b^2/a using (A.4.1):

$$\frac{b^2}{a} = \frac{\Lambda^2}{2\gamma} \frac{\left(k^2 - k^4 \frac{\lambda}{\Lambda}\right)^2}{1 + k^2 \frac{\sigma}{\gamma} + k^4 \frac{\kappa}{\gamma}} = \frac{\Lambda^2}{2\gamma} \left(k^4 - k^6 \left(-2\frac{\lambda}{\Lambda} - \frac{\sigma}{\gamma} \right) \right) + \mathcal{O}(k^8) \tag{3.1.4}$$

At this point it is useful to compare (3.1.4) to the very similar result in (2.6.3). There are **two** main differences:

1. The leading term is now $\mathcal{O}(k^4)$ instead of $\mathcal{O}(k^2)$, confirming our suspicion that some behaviour got shifted to higher orders. We will see that this leads to the necessity of including corrections up to order $\mathcal{O}(k^6)$ to secure stability.

2. Since the leading term in the denominator is now γ instead of σ, the "critical value" of Λ will now no longer depend on σ, but on γ. All dependence on λ, σ or κ lies in terms of order higher than four and will therefore not appear in the end result.

We thereby see the new Hamiltonian

$$H'_{\text{eff}} = \sum_k \left\{ \frac{k^2}{2} \beta + \frac{k^4}{2} \left(A - \frac{\Lambda^2}{\gamma} \right) \right\} + \mathcal{O}(k^6) \tag{3.1.5}$$

up to forth order in k. Transferring this to position space we get

$$\boxed{\mathtt{H}'_{\text{eff}} \approx \int \mathrm{d}^d x \left[\frac{B'}{2} (\nabla \phi)^2 + \frac{C'}{2} \left(\nabla^2 \phi \right)^2 + \frac{a_2}{2} \phi^2 + \frac{a_4}{2} \phi^4 - \mu \phi \right]} \quad \text{with} \quad B' = \beta \quad C' = A - \frac{\Lambda^2}{\gamma} \tag{3.1.6}$$

where we marked the new constants as B' and C'. Comparing this to (2.6.5), we see that $B' > 0$, but C' may change its sign in a similar manner to B by increasing $\Lambda \geq \Lambda'_c := \sqrt{A\gamma}$. Computing

σ_k similarly to (2.7.1) yields

$$\boxed{\sigma_k = -a_2 k^2 - B' k^4 - C' k^6} \tag{3.1.7}$$

which is now ill-behaved. This does not lead to pattern-forming behaviour, since either all growth rates are negative or after some $k_{\text{crit.}}$ all growth rates are positive and grow indefinitely. It is obvious that by including the $\frac{\gamma}{2} l^2$ term we shifted the interesting behaviour to a higher order in k. For dealing with this extra term, we should include terms in the Hamiltonian up to order $\mathcal{O}(k^6)$.

3.2 Including Higher Order Terms

If we want to include higher order terms for the rate of growth, it is a must to start with a Hamiltonian already containing higher order terms. For the new terms we demand that

(a) every term only contains two fields to keep the exact Gaussian structure.

(b) the Hamiltonian should be $\mathbb{Z}_2$ invariant.

This permits (up to shifts of the derivative operators) three new terms of order $\mathcal{O}(k^6)$:

$$H_{\text{new}} = \int \mathrm{d}^d x \left\{ \eta \left(\nabla^3 l\right)^2 + \zeta \left(\nabla^3 \phi\right)^2 + \chi \phi \left(\nabla^6 l\right) \right\} \tag{3.2.1}$$

This transfers to momentum space as given in A.2. We again calculate H_{eff} by writing

$$\begin{aligned} H = \sum_k \Big\{ & l_k l_k^* \left(\gamma + k^2\sigma + k^4\kappa + k^6\eta\right)/2 + \left(\phi_k l_k^* + l_l \phi_k^*\right)\left(-k^2\Lambda + k^4\lambda - k^6\chi\right)/2 \\ & + \phi_k \phi_k^* \left(k^2\beta + k^4 A + k^6\zeta\right)/2 \Big\} \\ = \sum_k & \left(\sqrt{a} l_k + \frac{b}{\sqrt{a}}\phi_k\right) \cdot \left(\sqrt{a} l_k + \frac{b}{\sqrt{a}}\phi_k\right)^* + \left(c - \frac{b^2}{a}\right)\phi_k \phi_k^* \end{aligned} \tag{3.2.2}$$

with $a = (\gamma + \sigma k^2 + \kappa k^4 + k^6\eta)/2$, $b = (\lambda k^4 - \Lambda k^2 - \chi k^6)/2$ and $c = (\beta k^2 + A k^4 + \zeta k^6)/2$. We expand b^2/a, now up to sixth order in k using (A.4.1) to arrive at

$$\frac{b^2}{a} = \frac{\Lambda^2}{2\gamma} \frac{\left(k^2 - k^4 \frac{\lambda}{\Lambda} + k^6 \frac{\chi}{\Lambda}\right)^2}{1 + k^2 \frac{\sigma}{\gamma} + k^4 \frac{\kappa}{\gamma} + k^6 \frac{\eta}{\gamma}} = \frac{\Lambda^2}{2\gamma}\left(k^4 + k^6\left(-2\frac{\lambda}{\Lambda} - \frac{\sigma}{\gamma}\right)\right) + \mathcal{O}(k^8) \tag{3.2.3}$$

and thereby see

$$H'_{\text{eff}} = \sum_k \frac{k^2}{2}\beta + \frac{k^4}{2}\left(A - \frac{\Lambda^2}{\gamma}\right) + \frac{k^6}{2}\left(\zeta + 2\frac{\lambda\Lambda}{\gamma} + \sigma\frac{\Lambda^2}{\gamma^2}\right) \tag{3.2.4}$$

and the full effective Hamiltonian in position space is

$$\boxed{\mathtt{H}'_{\text{eff}} \approx \int \mathrm{d}^d x \left[\frac{B'}{2} \left(\nabla\phi\right)^2 + \frac{C'}{2} \left(\nabla^2\phi\right)^2 + \frac{D'}{2} \left(\nabla^3\phi\right)^2 + \frac{a_2}{2}\phi^2 + \frac{a_4}{2}\phi^4 - \mu\phi \right]} \quad \text{with} \quad B' = \beta \qquad C' = A - \frac{\Lambda^2}{\gamma} \qquad D' = \zeta + 2\frac{\lambda\Lambda}{\gamma} + \sigma\frac{\Lambda^2}{\gamma^2} \tag{3.2.5}$$

up to sixth order in momentum. Calculating σ_k in the manner of (2.7.1) yields

$$\boxed{\sigma_k = -a_2 k^2 - B' k^4 - C' k^6 - D' k^8} \tag{3.2.6}$$

With this we recover the structure of the results of [Kai22]. Now not only the k^2 terms, but the terms up to k^4 let σ_k decrease with increasing k. For certain parameter-combinations, i.e. $\Lambda \geq \Lambda'_c = \sqrt{A\gamma}$ the sign of C' becomes negative (c.f. the previous case where $\Lambda \geq \Lambda_c = \sqrt{\beta\sigma}$ allowed for a sign change), therefore allowing an increase of σ_k at intermediate k. For $D' > 0$ this increase will stop and for large k the rates of growth will decrease again. This can lead to a finite region $[k_{\min}, k_{\max}]$ in which the modes ϕ_k have positive rate of growth σ_k, therefore resembling the behaviour of rates of growth in pattern formation as in Fig. 2.3.
We discover that in the end result the dependence on κ is lost, as it is found in the next higher order. We therefore see that the introduction of the γ-term had two effects comparing to (2.6.5):

1. It shifted the **dependencies** of the behaviour of $\sigma(k)$ from $\sigma \to \gamma$ and $\kappa \to \sigma$ "two orders in k down". So the term deciding whether or not we see an increase of σ_k towards intermediate k is in both cases "controlled" by the "lowest order" parameter in the Hamiltonian of l, being $\sigma\left(\nabla l\right)^2$ in the original Leibler & Andelman Hamiltonian and γl^2 in the new Hamiltonian.

2. The **behaviour** got shifted to a higher order in momenta, as γ penalises deviations from a flat membrane more severely than terms of higher order in momenta. For a large system of size $\sim L$, even if the deviation l from the reference height $l_0 = 0$ is large compared to other relevant quantities in the system, the gradient might still be small of order $\sim l/L \ll 1$.

The new system, described by the modified Hamiltonian (3.2.5), therefore (at least under the aspect of pattern formation) behaves similarly to the original Leibler & Andelman Hamiltonian (2.5.4) when one includes terms of the next higher order. We therefore found the additional term to be irrelevant, and it may therefore be omitted from the Hamiltonian if one is only interested in the qualitative behaviour. This is encouraging, because the measurements of the constants in momentum order $\mathcal{O}(k^6)$ or higher become ever more difficult.

Chapter 4

Mode Coupling and Growth Regulation

The results of [Kai22], that lipid bilayers may indeed be described by a demixing model, leave two further questions unanswered:

1. What mechanism is responsible for the modes ϕ_k with positive σ_k not growing to infinity?
2. Looking at Figure 1.3, we see very sharp patterns. But if multiple modes ϕ_k have positive rate of growth, we should expect the patterns to "smear out". Is there a mechanism that leads to a selection of modes in momentum space and thereby sharpens the pattern?

We will answer both questions and show that the neglected term $a_4\phi^3$ in calculating the rate of growth in 2.7 serves as the mechanism to dampen the growth of the modes. It is then this mechanism that also leads to the development of only one growing mode in the entire system, thereby leading to the formation of a sharp pattern.

4.1 Getting the Time Evolution Equation

We will again proceed to work in momentum space. As stated in (A.3.12), the time evolution of the mode ϕ_q in momentum space is given by

$$\boxed{\partial_t \phi_q = \sigma_q \phi_q - A_q \sum_{r,l} \phi_l \phi_r \phi_{q-r-l}} \tag{4.1.1}$$

where we defined $A_q := \frac{Mq^2 a_2}{2L}$ with L being the system size, so an area in $2d$. While we know the precise definition of σ_q, for all that is following it suffices to assume σ_q to be positive only in a finite region, i.e.

$$\sigma_k > 0 \Leftrightarrow k \in [k_{\min}, k_{\max}] \tag{4.1.2}$$

r	s	k-r-s
k	k	-k
k	-k	-k
-k	k	k
-k	-k	3k

Table 4.1: All possible index-combinations leading to terms of leading order in the sum in (4.1.1) for the time evolution of the dominant mode with positve σ_k. The *terms* are not of leading order.

which is fulfilled as was shown by [Kai22]. The key to developing the mechanism of mode dampening lies in approximating the nonlinear term in (4.1.1). The main ingredient is that the modes are discrete because we are in a finite volume. As the characteristic feature of σ_k is that only in a region $[k_{\min}, k_{\max}]$ the rate of growth is positive, we can assume that only $1, 2, \dots$ up to n modes have a positive linear rate of growth σ_k. We can then work our way up to arbitrary many modes with positive rate of growth, starting from $n = 1$.
To be explicit, we will look at the case of one mode with positive σ_k to understand the characteristic features of the mechanism that dampens the rate of growth and to see how resonances emerge. We will then look at the case for two modes with positive σ_k to see how the system achieves only one macroscopic mode in the end. After that we will jump to n modes with positive σ_k to show the previous results to extend to arbitrary many modes.
The idea now is that the modes with positive rate of growth will be substantially larger than the ones with negative σ_k.

4.2 One Mode with Positive Growth

The simplest case is that of only one dominant mode. Since this is the case in which we may calculate everything explicitly with a reasonable amount of work, we try to be as explicit as possible in order to gain understanding of what needs to be done in cases of multiple dominant modes.
In the current case, only one mode ϕ_k has positive rate of growth, while all other modes ϕ_q have non-positive growth:

$$\sigma_k > 0, \quad \sigma_q < 0 \; \forall q \neq k \tag{4.2.1}$$

We therefore assume that the sum in (4.1.1) is dominated by the terms of highest order in ϕ_k.

4.2.1 Growth of Dominant Mode

If we look at the time evolution for the only mode ϕ_k with positive σ_k, the sum in (4.1.1) is dominated by the $\phi_k|\phi_k|^2$ term, since this term is of highest order in the dominant modes, see

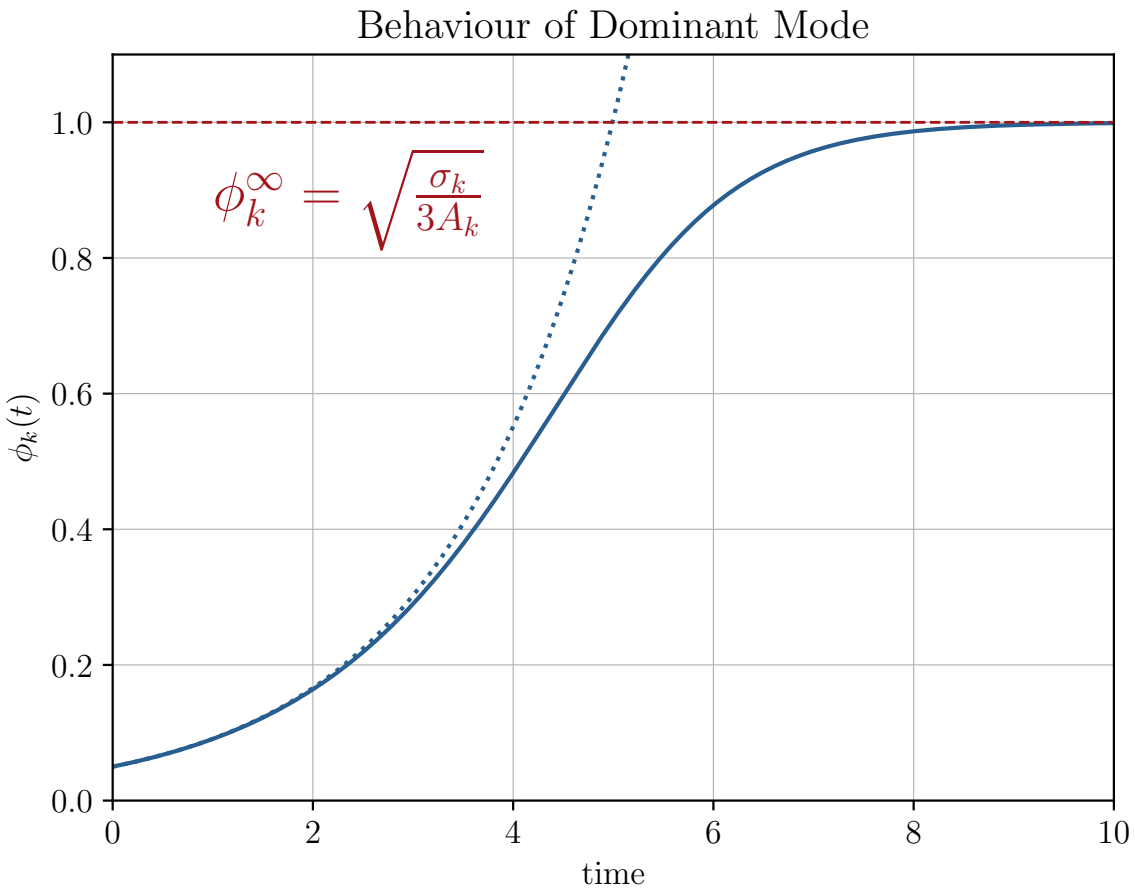

Figure 4.1: The growth of the dominant mode. For later times it approaches the red line, marking the value of ϕ_k^∞. For earlier times, marked by the dotted blue line, the growth is approximately exponential, as should be the case. For this plot a rate of growth of $\sigma_k = 0.6$ was used.

tab. 4.1. We find

$$\sum_{r,l} \phi_r \phi_l \phi_{k-r-l} \approx 3\phi_k |\phi_k|^2 \tag{4.2.2}$$

and therefore

$$\boxed{\partial_t \phi_k \approx \left(\sigma_k - 3A_k |\phi_k|^2\right) \phi_k} \tag{4.2.3}$$

This equation is solved (up to a complex phase we set to zero) by

$$\boxed{\phi_k(t) = \phi_k^\infty \cdot \frac{\exp\left(\sigma_k t\right)}{\sqrt{\exp\left(2\sigma_k t\right) + \left[\frac{\phi_k^\infty}{\phi_k^0}\right]^2 - 1}}} \tag{4.2.4}$$

r	s	q-r-s
k	k	q-2k
k	-k	q
-k	k	q
-k	-k	q+2k
k	q	-k
-k	q	k
k	*-q*	*2q-k*
-k	*-q*	*2q+k*

Table 4.2: All possible index-combinations leading to terms of leading order in the sum (4.1.1) for the time evolution of the non-dominant modes with $\sigma_q \leq 0$. The *terms* are of sub-leading order. The terms below the double bar appear twice because of the $k \leftrightarrow q$ symmetry.

where ϕ_k^∞ is the value of ϕ_k that is approached when $t \to \infty$ and ϕ_k^0 is the value of $\phi_k(t)$ at $t = 0$. The calculation leading up to (4.2.4) can be seen in A.9. The graph of (4.2.4) can be seen in Fig. 4.1. For small t it behaves like

$$\phi_k(t) \approx \phi_k^0 \exp(\sigma_k t) \tag{4.2.5}$$

growing exponentially. This should be the case since [Kai22] did this calculation in a small ϕ approximation. This gives us the right to call σ_k the rate of growth. But for larger times[1]

$$t \gtrsim \frac{1}{\sigma_k} \ln\left(\sqrt{\left(\frac{\phi_k^\infty}{\phi_k^0}\right)^2 - 1}\right) \approx \frac{1}{\sigma_k} \ln\left(\phi_k^\infty / \phi_k^0\right) \tag{4.2.6}$$

the behaviour changes and a dampening takes place. The end-magnitude $\lim_{t\to\infty} \phi_k(t) := \phi_k^\infty$ is found by setting the parenthesis in (4.2.3) to zero

$$\boxed{|\phi_k^\infty|^2 = \frac{\sigma_k}{3A_k}} \tag{4.2.7}$$

This result will be rather important in the end, as it is the final magnitude of **any non-vanishing** mode with positive rate of growth, independent of the number of modes with positive rate of growth, as we will show further on.

4.2.2 Growth of Non-Dominant Modes

The next case we need to look at is the growth of all the "non-dominant" modes ϕ_q, i.e. modes with $\sigma_q < 0$. The sum in (4.1.1) is now dominated by terms that include two factors of ϕ_k

[1] The approximation is for $\phi_k^\infty \gg \phi_k^0$.

instead of three. As can be seen in table 4.2, we have

$$\sum_{r,l} \phi_r \phi_l \phi_{q-r-l} \approx 6|\phi_k|^2 \phi_q + \phi_k^2 \phi_{q-2k} + \phi_k^{*2} \phi_{q+2k} \tag{4.2.8}$$

We now need to introduce some approximations:

- As long as $q \pm 2k \neq k$ (this case is dealt with later and leads to resonances) we can approximate $|\phi_q| \approx |\phi_{q-2k}|$ meaning that all non-dominant modes have approximately the same magnitude. Thereby we can write

$$\phi_{q\pm 2k} \approx \phi_q e^{i\Theta_\pm} \tag{4.2.9}$$

  with some phase $\Theta_\pm$.

- Since Θ (especially for more than one mode with positive σ_k) depends on multiple different modes and their phase relations to ϕ_q, we want to approximate Θ as a random variable.

Using the above approximations we write

$$\phi_k^2 \phi_{q-2k} + \phi_k^{*2} \phi_{q+2k} \approx R e^{i\vartheta} \cdot 2|\phi_k|^2 \phi_q \tag{4.2.10}$$

where $0 \leq R \leq 1$ is a random variable as well as $0 \leq \vartheta < 2\pi$. Inserting (4.2.10) and (4.2.8) into (4.1.1) for the case of a mode ϕ_q with negative σ_q yields

$$\boxed{\partial_t \phi_q = \left(\sigma_q - A_q \left[6 + 2R\cos(\vartheta)\right] |\phi_k|^2\right) \phi_q - i2A_q |\phi_k|^2 R \sin(\vartheta) \phi_q} \tag{4.2.11}$$

This equation has some very easy interpretations and in the end we will see that the behaviour for the non-dominant modes for arbitrary many modes with positive rate of growth will always fall back to this case of only one dominant mode.
Following A.5 the magnitude of ϕ_q is determined by the real part of (4.2.11). Per definition $\sigma_q < 0$, and since $0 \leq R \leq 1$ and $-1 \leq \cos(\vartheta) \leq 1$ we know that $6 + 2R\cos(\vartheta) > 0$ and thereby $\sigma_q - A_q \left[6 + 2R\cos(\vartheta)\right] |\phi_k|^2 < 0$ independent of the value of the random variables. ϕ_q is decreasing, though the rate at which this happens may vary.
The imaginary part of (4.2.11) determines the phase of ϕ_q. This part is only dependant on the variables approximated as random, and thereby behaves randomly, which is consistent with our approximation.
Therefore, the non-dominant modes behave as follows:

- The phase rotates stochastically.

- The magnitude is always decreasing, though the rate may vary, depending on the random noise through the mode-coupling.
- After having reached $|\phi_q| \approx 0$, small and short-lived deviations from zero may only appear because of higher order corrections.

As we will see later, the only stable solution of the system is that of **only one** mode ϕ_k with a much larger magnitude than all other modes. Therefore the behaviour of the non-dominant modes will always fall back to the case discussed here.

4.2.3 Resonances

As mentioned in the approximations taken in 4.2.2, we excluded the case $q + 2k = k$ and $q - 2k = k$. The first case simply means that $q = -k$, but since everything is symmetric in $k \leftrightarrow -k$ this has already been dealt with. In the second case, a term of order ϕ_k^3 appears in the approximation of the sum in (4.1.1) and dominates the approximation:

$$\partial_t \phi_q = \left(\sigma_q - 6A_q|\phi_k|^2\right)\phi_q - A_q\phi_k^3 + \text{Rnd.} \tag{4.2.12}$$

We abbreviated the random terms in equation (4.2.12). If we assume the stochastic effects influencing the magnitude to be small and have mean zero, we can look for stable solutions of (4.2.12) by setting $\partial_t \phi_q = 0$ and ignoring the random terms. This leads to

$$|\phi_q| = \frac{A_q|\phi_k|^2}{\sigma_q - 6A_q|\phi_k|^2}|\phi_k| \tag{4.2.13}$$

For late times $t \to \infty$ we may replace $|\phi_k|^2$ by $|\phi_k^\infty|^2 = \frac{\sigma_k}{3A_k}$ as given in (4.2.7) leading to

$$\boxed{|\phi_q^\infty| = \frac{1}{3}\frac{1}{2 - \frac{\sigma_q}{\sigma_k}\frac{A_k}{A_q}}|\phi_k^\infty|} \tag{4.2.14}$$

and the **resonant modes** have a finite final magnitude instead of a vanishing one.
In the case of only one mode with positive rate of growth it is reasonable to assume that $|\sigma_q| \gg |\sigma_k|$, since σ_k is positive but still small in magnitude, whilst σ_q is very negative. Then we may approximate the fraction and get

$$\boxed{|\phi_{q=3k}^\infty| \approx 3\frac{\sigma_k}{|\sigma_q|}|\phi_k^\infty|} \tag{4.2.15}$$

where we used that $A_q/A_k = 9$ if $q = 3k$. It is however important that the approximation $|\sigma_q| \gg |\sigma_k|$ may break down in the case of many modes with positive rate of growth, since then σ_k may be large in terms of its magnitude.
This result is quite nice, as we see that the resonant modes are only scaled versions of the dominant mode, with the scaling factor being the ratio of the rates of growth (up to a combinatorical factor). This is in some way to be expected in processes of pattern formation. Haken called this behaviour (that some degrees of freedom are simply scaled versions of other "macroscopic" degrees of freedom) "mode-enslavement" [Hak77].
Because the $q = 3k$ mode is non vanishing, the mode $q' = q + 2k = 5k$ will also show resonant behaviour, coupling to the previous resonant mode. This will lead to a cascade of non-vanishing "resonant" modes with (approximately[2]) exponentially decreasing magnitude. In the approximation of (4.2.15) we see that the $q = (2N + 1)k$ mode has final magnitude

$$|\phi_q^\infty| = \frac{(2N+1)^2}{3} \frac{\sigma_k}{|\sigma_q|} |\phi_{q-2k}^\infty| \tag{4.2.16}$$

leading to the expectation of some "echoes" of small magnitude of the dominant mode in momentum space.

4.3 Two Dominant Modes

The case of one dominant mode will serve as the basis of the analysis, as in the end (at least in some approximation) all behaviour will revert to this case. The case we will now study, of two modes ϕ_k and ϕ_l with positive rate of growth, $\sigma_k, \sigma_l > 0$, serves to introduce to us the principles that will cause every mode up to one to vanish in the end. This means that we will only need to look at the behaviour of the dominant modes, as the behaviour of the modes with negative σ_q and the behaviour of the resonances should be the same as in the previous section. As this mainly has the purpose to illustrate the principles we employ in the generalisation, we try to be very explicit in what we are doing.
Let us therefore assume that the two neighbouring modes ϕ_k and ϕ_l with $l = k+1$ have positive rate of growth and therefore dominate the sum in (4.1.1). One may now list all combinations of indices that lead to terms of leading order in the dominant modes, as has been done in table 4.3. We then see that the sum in (4.1.1) for the evolution of the mode k is approximated in leading order by

$$\sum_{r,s} \phi_r \phi_s \phi_{k-r-s} \approx \left(3|\phi_k|^2 + 6|\phi_l|^2\right) \phi_k \tag{4.3.1}$$

[2]The magnitude decreases only approximately exponentially because of the factor arising from $A_q/A_{q'}$ and the changing value of σ_q for different q.

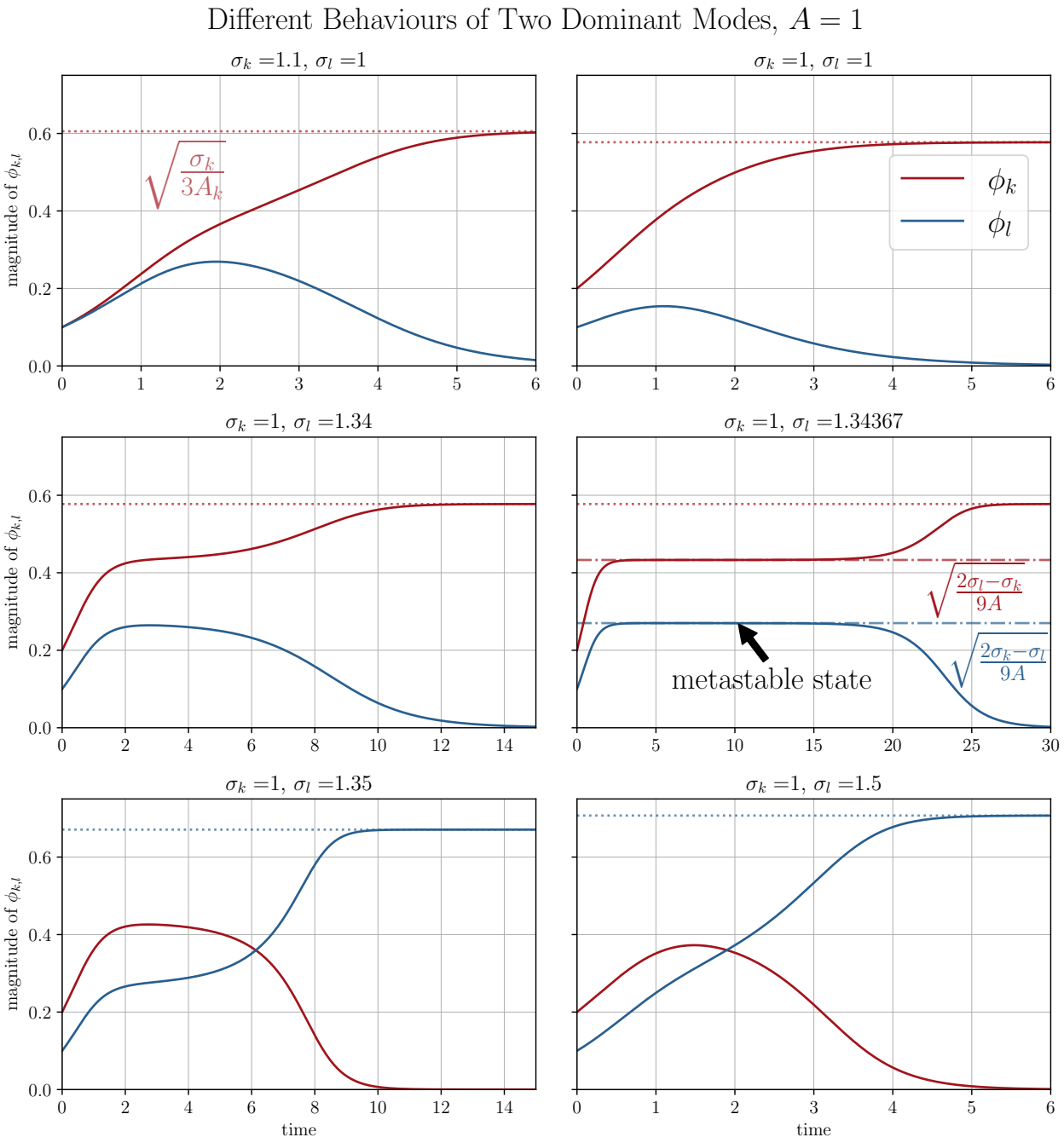

Figure 4.2: If two modes have positive rate of growth, their behaviour over time may vary depending upon the initial conditions, i.e. at what magnitude they start and what their respective rate of growth is. In all cases one mode goes to zero. The non-vanishing mode approaches the value ϕ^∞ from the previous case, indicated by the dotted line. The mode that dominates is not always the initially larger one. The last four graphs depict a situation in which the mode with the initially smaller magnitude has the larger rate of growth. At some value of σ_l the behaviour changes and the l mode ends up becoming the non-vanishing one. During this, a metastable state may appear for a limited time in which both solutions approximately do not change their value.

r	s	k-r-s
k	k	-k
k	-k	k
-k	k	k
-k	*-k*	*3k*
l	*l*	*k-2l*
l	-l	k
-l	l	k
-l	*-l*	*k+2l*
k	l	-l
k	-l	l
-k	*l*	*2k-l*
-k	*-l*	*2k+l*

Table 4.3: All index-combinations leading to terms of leading order in the dominant modes in the sum in (4.1.1) for the time-evolution of the dominant mode ϕ_k (hence the asymmetry between k and l). All *terms* are of sub leading order. All terms below the double bar appear twice because of the possible $k \leftrightarrow l$ exchange.

The asymmetry between k and l arises because this is the evolution for ϕ_k. The equivalent equation for ϕ_l is asymmetric the other way round. The two evolution equations for ϕ_k and ϕ_l therefore are

$$\boxed{\begin{aligned}\partial_t\phi_k =&\sigma_k\phi_k - A_k\left(3|\phi_k|^2 + 6|\phi_l|^2\right)\phi_k\\ \partial_t\phi_l =&\sigma_l\phi_l - A_l\left(3|\phi_l|^2 + 6|\phi_k|^2\right)\phi_l\end{aligned}} \tag{4.3.2}$$

These equations represent a set of coupled differential equations, and one may already guess the necessarily arising symmetry in these equations after approximating $A_k \approx A_l$. The possible behaviours that may arise from (4.3.2) are depicted in Fig. 4.2. The first obvious realisation is that in all cases, eventually one mode vanishes. The non-vanishing mode approaches the value $\sqrt{\frac{\sigma_X}{3A_X}}$, which was the final value ϕ_X^∞ calculated for the case of only one dominant mode.
The first two cases show that from two equal modes, the one with either the larger initial value or rate of growth will "win" over the other, while the other mode will vanish.
The next four cases show the k mode with larger initial value, but the l mode with substantially larger rate of growth. At first, the k mode still "wins" over the l mode. At around $\sigma_l \approx 1.34367\ldots$ the behaviour changes, and now the l mode dominates after some time and the k mode vanishes. When σ_l approaches the value at which the behaviour changes, a metastable state may appear, i.e. that both modes seem to not change their magnitude for some time, but then still depart in different directions. The value of the metastable magnitudes is written beside them.
As one may conclude from the graph (and as we prove down below) this metastable state

is unstable. Both modes should depart rather quickly. But around precisely the right value of $\sigma_l = 1.34367\ldots$ this departure takes increasingly longer. This might be associated with something like "critical slowing down" or a bifurcation, as the time needed for the system to depart from the metastable state becomes longer and longer while the behaviour (i.e. what mode is the non-vanishing one) of the system changes.
Going further, we do not try to solve the equations (4.3.2) directly, but are rather interested in the possible stable solutions, i.e. solutions ϕ_k & ϕ_l that obey $\partial_t\phi_k = \partial_t\phi_l = 0$. Because of the symmetry of the equations one immediately sees three different types of solutions:

1. $\phi_k = \phi_l = 0$
   This obviously satisfies $\partial_t\phi_k = \partial_t\phi_l = 0$. But this solution is unstable, as can be seen without further analysis. Since for small ϕ one may disregard the cubic term in ϕ, every deviation from $\phi = 0$ leads to a positive rate of growth and thereby increases the deviation further.

2. Only **one non-vanishing** mode.
   Without loss of generality, we choose $\phi_k = 0$ and $\phi_l \neq 0$. In this case the equation for ϕ_l in (4.3.2) reduces to the case of only one dominant mode (4.2.3), for which we already know the stable final magnitude of ϕ_l is given by (4.2.7), that is to say in this case

   $$|\phi_k|^2 = 0, \quad |\phi_l^\infty|^2 = \frac{\sigma_l}{3A_l}$$

   The important aspect to understand about this case is that if all but one mode vanish, all equations (also for the non-dominant modes) must naturally revert to the case of 4.2 i.e. to the case of only one dominant mode. The simulations depicted in Fig. 4.2 already suggest that this solution is favoured by the system. The final magnitudes described above are the ones shown in the figure.

3. $\phi_k \neq 0 \neq \phi_l$
   In this case we may solve (4.3.2) for the final magnitudes and get

   $$\begin{aligned} |\phi_k^\infty|^2 &= \frac{2\sigma_l - \sigma_k}{9A} \\ |\phi_l^\infty|^2 &= \frac{2\sigma_k - \sigma_l}{9A} \end{aligned} \tag{4.3.3}$$

   where we already approximated $A_q \approx A_k := A$ (see A.7 for the range of validity of the approximation). This set of solutions is unstable, as we will show below. But interestingly these are the magnitudes of the metastable states in Fig. 4.2. We thereby see that the system might approach this solution but will depart shortly after and approach the stable

solution above. Whilst we could do the rigorous mathematical analysis on the stability of this solution, it might be better to first gain some intuition on why it should make sense that such a solution should not be stable.

Because in the equation for $\partial_t \phi_k$ in (4.3.2) the term proportional to $|\phi_l|^2$ appears with a larger factor (here twice) than the $|\phi_k|^2$ term, the rate of growth for σ_l dominates the growth of ϕ_k! This would mean that the mode with the **smaller** linear rate of growth eventually grows **larger** than the mode with the higher rate of growth. This seems not only paradoxical, but it is indeed (as we will show below) unstable. But there is a thing to take away here: Because of the symmetry between the equations for multiple (here only two) dominant modes, in the equation for $\partial_t \phi_k$ the terms proportional to **other modes** $|\phi_q|^2$ with $q \neq k$ will **always** appear with larger factors than the terms proportional to $|\phi_k|^2$. In the end, this will be the reason why only the case with one non-vanishing mode is stable.

4.4 Linear Stability Analysis

To get a rigorous result about the stability of the types of solutions mentioned above, we need to perform a linear stability analysis (see A.8). After performing some general steps we will look at the explicit results, thereby showing that the third case is unstable whilst the second case is stable and therefore the only stable solution of the system. We therefore simplify the equations (4.3.2) by approximating[3] $A_q \approx A_k := A$, setting $x := \phi_k$ and $y := \phi_l$, writing $\sigma_x := \frac{\sigma_k}{3A}$, $\sigma_y := \frac{\sigma_l}{3A}$ and finally scaling the time as $t \to 3At$ leading to

$$\begin{aligned} \dot{x} &= x\sigma_x - \left(x^2 + 2y^2\right) x \\ \dot{y} &= y\sigma_y - \left(y^2 + 2x^2\right) y \end{aligned} \tag{4.4.1}$$

If we want to analyse the stability of a solution $\boldsymbol{x}_0 = (x_0, y_0)^\top$ we substitute $\boldsymbol{x} = \boldsymbol{x}_0 + \delta\boldsymbol{x}$ with the condition $\partial_t \boldsymbol{x}_0 = 0$. This leads to

$$\begin{aligned} \delta\dot{x} &= \left(\sigma_x - \left(x_0^2 + 2y_0^2\right)\right) \delta x - 2x_0^2 \delta x - 4x_0 y_0 \delta y \\ \delta\dot{y} &= \left(\sigma_y - \left(y_0^2 + 2x_0^2\right)\right) \delta x - 2y_0^2 \delta y - 4x_0 y_0 \delta x \end{aligned} \quad \Leftrightarrow \quad \boxed{\delta\dot{\boldsymbol{x}} = M \times \delta\boldsymbol{x}} \tag{4.4.2}$$

where we used the equivalent matrix formulation on the right with

$$M := \begin{pmatrix} \sigma_x - (x_0^2 + 2y_0^2) - 2x_0^2 & -4x_0 y_0 \\ -4x_0 y_0 & \sigma_y - (y_0^2 + 2x_0^2) - 2y_0^2 \end{pmatrix} \tag{4.4.3}$$

[3] More on the validity of this approximation in A.7.

whilst we have to remember that per definition of $\boldsymbol{x}_0$

$$\boxed{\left(\sigma_x - \left(x_0^2 + 2y_0^2\right)\right) x_0 = 0} \quad \text{and} \quad \boxed{\left(\sigma_y - \left(y_0^2 + 2x_0^2\right)\right) y_0 = 0} \tag{4.4.4}$$

The solution $\boldsymbol{x}_0$ is stable if M has only negative eigenvalues.

4.4.1 Stability of Two Non-Vanishing Modes

We want to analyse the set of solutions

$$x_0^2 = \frac{2\sigma_y - \sigma_x}{3} \neq 0 \quad \text{and} \quad y_0^2 = \frac{2\sigma_x - \sigma_y}{3} \neq 0 \tag{4.4.5}$$

which satisfy $\dot{x}_0 = \dot{y}_0 = 0$. Because the solution is assumed to be different from zero, we get from (4.4.4) that

$$\sigma_x = x_0^2 + 2y_0^2 \quad \text{and} \quad \sigma_y = y_0^2 + 2x_0^2 \tag{4.4.6}$$

which is the crucial step for simplifying the matrix M. Using (4.4.6) we know

$$M = -2 \begin{pmatrix} x_0^2 & 2x_0y_0 \\ 2x_0y_0 & y_0^2 \end{pmatrix} := -2D \tag{4.4.7}$$

For more clarity later on we already use the **Sylvester-criterion** (see A.6) to prove that D is **not positive semi-definite**, i.e. has at least one eigenvalue $\lambda < 0$ and thereby M has at least one positive eigenvalue and the solution is unstable.
The upper left 2×2 sub-determinant of D is simply the determinant of D:

$$|D| = x_0^2y_0^2 - 4x_0^2y_0^2 = -3x_0^2y_0^2 < 0 \tag{4.4.8}$$

because we assumed $x_0, y_0 \neq 0$. Thereby D is not positive semidefinite and therefore M has at least one positive eigenvalue, which makes the solution $x_0 \neq 0 \neq y_0$ unstable.

4.4.2 One Non-Vanishing Mode

We can also analyse the case of only one unstable mode, w.l.o.g. $x_0 = \sqrt{\sigma_x} \neq 0$ and $y_0 = 0$. In this case M becomes diagonal with

$$M = \begin{pmatrix} \sigma_x - 3x_0^2 & 0 \\ 0 & \sigma_y - 2x_0^2 \end{pmatrix} = -2 \begin{pmatrix} \sigma_x & 0 \\ 0 & \sigma_x - \frac{\sigma_y}{2} \end{pmatrix} := -2D \tag{4.4.9}$$

We read of that D has eigenvalues $\left\{\sigma_x, \sigma_x - \frac{\sigma_y}{2}\right\}$ and therefore the solution is stable if $\sigma_x > \frac{\sigma_y}{2}$. This means, the solution that the mode with the largest rate of growth is non-vanishing whilst all others vanish is **always stable**! But if the rates of growth do not differ too drastically from one another then also a mode with a lower rate of growth may become the non-vanishing one. This could already be seen in Fig. 4.2.

4.5 Arbitrary Many Modes

We now analyse the case of arbitrary many modes ϕ_{x_i} with positive rates of growth $\sigma_{x_i} > 0$. The challenge here is to get the form of the matrix M from (4.4.2). After that the analysis works in the same way as it did for the case of only two non-vanishing modes. The task is to approximate the sum $\sum_{r,s} \phi_r \phi_s \phi_{q-r-s}$ in (4.1.1) for the growth of the q mode. What assumptions do we use?

- Since we look at the behaviour of the dominant modes, only terms of order three in the dominant modes are interesting for the approximation.
- We further assume that only terms of the form $\sim |\phi_j|^2 \phi_i$ (where $i = j$ is included) matter for the approximation. All other terms are explicitly dependant on a complex phase and will therefore contribute only to the **noise terms** (i.e. their explicit dependency on the complex phase will make them oscillate rapidly, therefore leading to an average zero influence) in the way we showed in the case of the non-dominant modes, 4.2.2.
- The implicit approximation in the previous step is that the noise-term is relatively unimportant compared to the "non-noise" terms. The approximation may therefore collapse if the noise becomes too large. The whole behaviour of the system may then become stochastic.

If one accepts these assumptions, only a handful of terms may contribute.
First of all we have terms in which only one index appears:

r	s	$x_i - r - s$	
x_i	x_i	$-x_i$	$\Rightarrow 3\|\phi_{x_i}\|^2 \phi_{x_i}$
x_i	$-x_i$	x_i	
$-x_i$	x_i	x_i	

The term with $r = s = -x_i$ is explicitly dependant on a complex phase and therefore does not appear.
Second we have terms in which another index appears twice. Those are

r	s	$x_i - r - s$	
x_j	$-x_j$	x_i	$\Rightarrow 2\sum_{j\neq i} \lvert\phi_{x_j}\rvert^2\phi_{x_i}$
$-x_j$	x_j	x_i	

and

r	s	$x_i - r - s$	
x_i	x_j	$-x_j$	$\Rightarrow 2\times 2\sum_{j\neq i} \lvert\phi_{x_j}\rvert^2\phi_{x_i}$
x_i	$-x_j$	x_j	

where the factor of 2 arises because one may swap $r \leftrightarrow s$. Look at tab. 4.3 to spot the similarities, now for "multiple j's".
Combining everything the equation of motion is

$$\partial_t \phi_{x_i} = \left(\sigma_{x_i} - 3A_{x_i}\left\{|\phi_{x_i}|^2 + 2\sum_{j\neq i}|\phi_{x_j}|^2\right\}\right)\phi_{x_i} + \text{Noise} \tag{4.5.1}$$

To simplify things we again write $\phi_{x_i} = x_i$, approximate $A := A_{x_i} \approx A_{x_j}$, write $\sigma_i := \frac{\sigma_{x_i}}{3A}$ and scale $t \to 3At$ to get

$$\partial_t x_i = \left(\sigma_i - \left\{x_i^2 + 2\sum_{j\neq i} x_j^2\right\}\right) x_i \tag{4.5.2}$$

Now everything follows the example of two dominant modes from 4.4. We expand around a set of solutions $x_{i,0}$ with $\partial_t x_{i,0} = 0$ to get

$$\delta\dot{x}_i = \left(\sigma_i - \left\{x_{i,0}^2 + 2\sum_{j\neq i} x_{j,0}^2\right\}\right)\delta x_i - 2x_{i,0}^2\delta x_i - 4x_{i,0}\sum_{j\neq i} x_{j,0}\delta x_j \tag{4.5.3}$$

with the constraint that

$$\left(\sigma_i - \left\{x_{i,0}^2 + 2\sum_{j\neq i} x_{j,0}^2\right\}\right) x_{i,0} \stackrel{!}{=} 0 \;\forall i \tag{4.5.4}$$

As a matrix-equation this becomes

$$\delta\dot{\boldsymbol{x}} = M \times \delta\boldsymbol{x} \tag{4.5.5}$$

with

$$M := \begin{pmatrix} (\sigma_1 - (x_{1,0}^2 + 2\sum_{j\neq 1} x_{j,0}^2)) - 2x_{1,0}^2 & -4x_{1,0}x_{2,0} & -4x_{1,0}x_{3,0} & \dots \\ -4x_{1,0}x_{2,0} & (\sigma_2 - (x_{2,0}^2 + 2\sum_{j\neq 2} x_j^2)) - 2x_{2,0}^2 & -4x_{2,0}x_{3,0} & \dots \\ -4x_{1,0}x_{3,0} & -4x_{2,0}x_{3,0} & (\sigma_3 - (x_{3,0}^2 + 2\sum_{j\neq 3} x_j^2)) - 2x_{3,0}^2 & \dots \\ \vdots & \vdots & \vdots & \ddots \end{pmatrix} \tag{4.5.6}$$

where we see that the resulting matrix M is **symmetric**, as is required by Sylvester's criterion. The necessary assumption for M being symmetric was the simplification of A.
We now prove two claims:

1. The solution with $x_i = \sqrt{\sigma_i} \neq 0$ and all other $x_j = 0$ for $j \neq i$ is stable as long as $\sigma_i > \frac{\sigma_j}{2}\ \forall j \neq i$.
2. Any solution with more than one $x_i \neq 0$ is unstable.

Ad 1

Let us assume w.l.o.g. that $x_{1,0} = \sqrt{\sigma_1} \neq 0$ and all other $x_j = 0$. Then M is diagonal

$$M = -2 \begin{pmatrix} \sigma_1 & \dots & \dots & \dots \\ \vdots & \sigma_1 - \frac{\sigma_2}{2} & \dots & \dots \\ \vdots & \vdots & \sigma_1 - \frac{\sigma_3}{2} & \dots \\ \vdots & \vdots & \vdots & \ddots \end{pmatrix} \tag{4.5.7}$$

and has only negative eigenvalues iff

$$\sigma_1 > \frac{\sigma_j}{2}\ \forall j \neq 1 \tag{4.5.8}$$

which completes the proof.

Ad 2

Let us assume that at least two values $x_{i,0}$ and $x_{j,0}$ are non-vanishing. We may swap rows and columns of the matrix M to get $i = 1$ and $j = 2$. As we do this with an even number of swaps, the determinant does not change. Because of (4.5.4) and the assumption that $x_{1,0} \neq 0 \neq x_{2,0}$, the first upper 2×2 sub-determinant of M looks like

$$M_{\text{sub}} = -2 \begin{pmatrix} x_{1,0}^2 & 2x_{1,0}x_{2,0} \\ 2x_{1,0}x_{2,0} & x_{2,0}^2 \end{pmatrix} := -2D_{\text{sub}} \tag{4.5.9}$$

with $\det(D_{\text{sub}}) = -3x_{1,0}^2 x_{2,0}^2 < 0$. Following the Sylvester-criterion from A.6, D has at least one negative eigenvalue, thereby M has at least one positive eigenvalue and the set of solutions is unstable.
We therefore know the results for two dominant modes to expand to an arbitrary number of dominant modes, i.e. that in any case, in the end only one mode will remain nonzero, as

all other modes will eventually vanish. In this process, metastable solutions of two (or more) nonzero modes that approximately do not change their magnitude for a finite amount of time may appear, but will vanish, as they are unstable and small perturbations will lead the solutions to diverge from one another.

Chapter 5

Summary & Outlook

In this thesis we looked at the interplay of the local curvature of a lipid bilayer and its local concentration. We focused our investigation on the effective model discussed by [LA87] in which the curvature field of the membrane was integrated out of the total Hamiltonian, containing curvature, concentration and coupling terms. Leibler & Andelman showed that this can lead to curvature induced instabilities in the concentration field, i.e. ordered modulations with a characteristic wavelength can emerge from homogeneous initial states. We took into consideration the results obtained by [Kai22], which show that the effective model developed by [LA87] is compatible with a demixing model. Such models are often used for lipids or conserved substances in general which usually lead to very coarse patterns with diverging wavelength (which is not observed for lipid bilayers), but in this case may show much finer patterns of (in principle) arbitrary wavelength, agreeing with observations.

We investigated the results obtained by [Kai22] under the addition of a new, zeroth order gradient term of the curvature field to the Hamiltonian. Such terms are often omitted, but can in principle lead to a different system behaviour. We found the introduction of such a term to make the approximation up to fourth order in momenta that Leibler & Andelman used insufficient to describe the effects found by [Kai22]. As a solution we calculated the effective Hamiltonian in an approximation up to sixth order in momenta. This introduced new constants of the system which are in practice not easy to measure as they are related to high momenta effects.

For the right values of these new parameters, the results of [Kai22] could be recovered, i.e. the concentration field can again undergo a linear instability and form modulations with arbitrary wavelength, depending on the values of the constants. Much of the dependencies found by [LA87] got shifted to higher momentum terms, but the approximation to higher order recovers them again. We have therefore shown the term introduced by us is not necessary to describe the qualitative behaviour of the system and might initially be omitted. The results of [LA87]

and others will therefore be at least qualitatively correct, even if such a term is present in the Hamiltonian. Still, for quantitative effects such a term might be necessary to include in the Hamiltonian description.
A natural next step would be to investigate how such higher order terms could be measured. Since the higher order approximation we calculated also allows the formation of patterns, one could estimate a range in which the newly introduced constants must be located in to reproduce the results e.g. found by [SA95]. After that, a comparison between the old and the new set of parameters would be in order. It is possible that the new set of constants would lead to the same results, only using more effort. Or there could be a difference in the two descriptions, favouring one over the other after comparison with the experiment.

In the second part we investigated what mechanism leads to the dampening of the initial exponential growth of the Fourier modes of the concentration field, as found by [Kai22], such that the modes do not grow to infinity. We showed the higher order mode coupling to be the key to dampen the growth. We systematically investigated scenarios with different numbers of (at first) growing modes and showed that in the end only one Fourier mode will be non-vanishing. During the system's development metastable states of multiple non-vanishing modes can appear for a short time for certain (fine tuned) parameter values. Besides the one non-vanishing mode multiple small "resonances" of said mode will appear in the system at multiples of the non-vanishing wave number. Their magnitude is proportional to that of the non-vanishing mode.
Since only one mode is non-vanishing, all behaviour of such systems can be discussed by looking only at the case of one mode with positive rate of growth, heavily simplifying the description of such systems in the non-linear regime. This is not only a simplification of the description, it also explains why patterns of such systems observed in nature appear sharp (cf. Fig. 1.3), even though a large band of modes might have positive rate of growth in momentum space. The selection of only one mode growing and all other modes vanishing leads to a δ-like distribution of mode-amplitudes in momentum space, thereby sharpening the patterns observed in vastly different systems (cf. Fig. 1.2). This analysis was only partly dependant on the results obtained in the first part, as we only assumed our rate of growth to be positive in a small range of wavelengths.
The first thing to build upon would be to investigate the assumptions used in developing our results. An important assumption was that only the terms of leading order in the growing modes are necessary for our system description. But for large systems, the sheer number of small modes might have a larger impact on the system than the small number of large modes. A criterion when such an assumption is appropriate is necessary. Furthermore the assumption

that the phase distribution of the different modes can be approximated as random needs to be checked. Especially the coupling of weakly growing modes, which we assumed as random with mean zero, has the potential to lead to other microscopically growing modes. If that is the case, their stability should be checked versus the naturally growing modes. One could also investigate whether or not such "resonances" we described are in fact found in systems. We showed that for fine tuned choices of parameters metastable states can appear. But we could not answer why in some cases the metastable state was approached and in others it was not (cf. Fig. 4.2). An analysis of these metastable states, maybe starting with the case of two growing modes as done in 4.3, is in order.

Appendix

A.1 Definitions and Conventions for the Fourier Transformation

We will only use transformations concerning the position-variables. Since we are dealing with finite volumes, we use the discrete Fourier transform with the conventions

$$\begin{aligned} f_n :=& \frac{1}{\sqrt{L}} \int_L \mathrm{d}x\, f(x) \exp\left(i k_n x\right) \\ f(x) :=& \frac{1}{\sqrt{L}} \sum_n f_n \exp\left(-i k_n x\right) \end{aligned} \tag{A.1.1}$$

and define $k_n := \frac{2\pi}{L} n$. For higher dimensions we use the natural extensions of (A.1.1). For the definition of the Kronecker-δ we use

$$\begin{aligned} \delta_{n,m} :=& \frac{1}{2\pi} \int_0^{2\pi} \exp\left(i(n-m)\phi\right) \mathrm{d}\phi = \frac{1}{L} \int_0^L \exp\left(2\pi i \left(\frac{n-m}{L}\right) \hat{\phi}\right) \mathrm{d}\hat{\phi} \\ =& \frac{1}{L} \int_L \exp\left(i(k_n - k_m)\hat{\phi}\right) \mathrm{d}\hat{\phi} \end{aligned} \tag{A.1.2}$$

and in the same way for the Dirac-δ

$$\delta(x-a) = \frac{1}{V} \sum_{n=-\infty}^{\infty} \exp\left(i k_n (x-a)\right) \tag{A.1.3}$$

A.2 Useful Formulae for Fourier Calculations

For $l \equiv l(x)$ and $\phi \equiv \phi(x)$ we will later use

$$\begin{aligned} \int \mathrm{d}^d x A \left(\nabla^n l\right)^2 &= \sum_k l_k l_k^* A k^{2n} \\ \int \mathrm{d}^d x A \phi \nabla^{2n} l &= (-1)^n \sum_k \frac{A}{2} \left(\phi_k l_k^* + l_k \phi_k^*\right) k^{2n} \end{aligned} \tag{A.2.1}$$

To revert back to position space we use

$$\sum_k \phi_k \phi_k^* \left(k^2 A + k^4 B\right) = \int \mathrm{d}^d x \left\{ \left(\nabla\phi\right)^2 A + \left(\nabla^2 \phi\right)^2 B \right\} \tag{A.2.2}$$

A.3 Calculating the Linear Rate of Growth

Here we explicitly look at Hamiltonians of the form

$$\begin{aligned} H &= \int \mathrm{d}^d x \left(\frac{B}{2} \left(\nabla\phi\right)^2 + \frac{C}{2} \left(\nabla^2\phi\right)^2 + \frac{a_2}{2}\phi^2 + \frac{a_4}{4}\phi^4 - \mu\phi \right) \\ &= \int \mathrm{d}^d x \left(\phi \frac{\left(-B\nabla^2 + C\nabla^4 + a_2\right)}{2} \phi + \frac{a_4}{4}\phi^4 - \mu\phi \right) \end{aligned} \tag{A.3.1}$$

which we can write more generally as

$$= \int \mathrm{d}^d x \left(\phi \frac{\mathcal{L}(\nabla^2)}{2} \phi + \frac{a_4}{4}\phi^4 - \mu\phi \right) \tag{A.3.2}$$

From $\mu = \frac{\delta H}{\delta \phi}$ follows

$$2\mu = \mathcal{L}(\nabla^2)\phi + a_4\phi^3 \tag{A.3.3}$$

The way to write $\mathcal{L}$ as a function of ∇^2 is in reference to [Hak77]. This has the advantage that in momentum space $\mathcal{L}$ is simply a function of $-k^2$. In the approach taken by [Kai22] we get $\partial_t \phi = M\nabla^2 \mu$ and thereby we see

$$\partial_t \phi = \frac{M\nabla^2}{2} \left(\mathcal{L}(\nabla^2)\phi + a_4\phi^3 \right) \tag{A.3.4}$$

In a small ϕ approximation, one may ignore the ϕ^3-term (thereby coining the term "linear rate of growth"), then transferring this to momentum space, again using the conventions in A.1, and

thereby see

$$\frac{1}{\sqrt{L}}\sum_k e^{-ikx}\left(\partial_t\phi_k(t)+k^2\frac{M}{2}\mathcal{L}(-k^2)\phi_k\right)=0 \tag{A.3.5}$$

For this to hold for any k, we need the parenthesis to vanish and thereby get the linear time evolution equation

$$\partial_t\phi_k(t)=\underbrace{\left[\frac{-k^2M}{2}\mathcal{L}(-k^2)\right]}_{:=\sigma_k}\phi_k=\sigma_k\phi_k \tag{A.3.6}$$

for the ϕ_k mode. This formalises how we calculate the rate of growth in the small ϕ approximation. In setting $M=1$ and discarding $\Delta\mu$, leading to an additional factor of 2 as done by [Kai22], one does not change the result qualitatively, which therefore might be done for convenience sake.

If we, instead of a small ϕ approximation, want to stay general, we may write

$$\phi(x,t)=\frac{1}{\sqrt{L}}\sum_k\phi_k(t)e^{-ikx}\quad\text{and}\quad\left(\mathcal{L}(\nabla^2)\phi+a_4\phi^3\right)=\frac{1}{\sqrt{L}}\sum_k\left(\mathcal{L}(\nabla^2)\phi+a_4\phi^3\right)_k e^{-ikx} \tag{A.3.7}$$

which leads to

$$\frac{1}{\sqrt{L}}\sum_k e^{ikx}\left(\partial_t\phi_k+\frac{k^2M}{2}\left(\mathcal{L}(\nabla^2)\phi+a_4\phi^3\right)_k\right)=0 \tag{A.3.8}$$

which has to hold for any k, giving us the time evolution equation in momentum space

$$\partial_t\phi_k=\frac{-k^2M}{2}\left(\mathcal{L}(\nabla^2)\phi+a_4\phi^3\right)_k \tag{A.3.9}$$

Now one has to calculate $\left(\mathcal{L}(\nabla^2)\phi+a_4\phi^3\right)_k$. The first part is linear and therefore the Fourier transformed is easy to find:

$$\begin{aligned}\left(\mathcal{L}(\nabla^2)\phi\right)_k=&\int\frac{\mathrm{d}^2x}{L}e^{ikx}\sum_q\mathcal{L}(\nabla^2)e^{-iqx}\phi_q\\=&\sum_q\delta_{q,k}\mathcal{L}(-q^2)\phi_q\\=&\mathcal{L}(-k^2)\phi_k\end{aligned} \tag{A.3.10}$$

where we used the definition of the Fourier transformed, inserted the transformation of ϕ and

used the definition of the Kronecker δ. The second part is a bit more tricky, but not much:

$$\begin{aligned}\left(a_4\phi^3\right)_k =& \int \frac{\mathrm{d}^2x}{L^2} e^{ikx} a_4 \sum_{q,r,l} \phi_q\phi_r\phi_l e^{-i(q+r+l)x} \\ =& \frac{a_4}{L}\sum_q \delta_{q,k-r-l} \sum_{r,l} \phi_q\phi_r\phi_l \\ =& \frac{a_4}{L}\sum_{r,l} \phi_r\phi_l\phi_{k-r-l}\end{aligned} \tag{A.3.11}$$

Plugging everything together leaves us with

$$\begin{aligned}\partial_t\phi_k =& \underbrace{\frac{-k^2M}{2}\mathcal{L}(-k^2)}_{\sigma_k}\phi_k - \underbrace{\frac{Mk^2a_4}{2L}}_{:=A_k}\sum_{r,l}\phi_r\phi_l\phi_{k-r-l} \\ \Rightarrow& \boxed{\partial_t\phi_k = \sigma_k\phi_k - A_k\sum_{r,l}\phi_r\phi_l\phi_{k-r-l}}\end{aligned} \tag{A.3.12}$$

as the time evolution equation for the k mode in momentum space. In general the definition for the linear rate of growth for the mode ϕ_k is

$$\boxed{\sigma_k = \frac{-k^2M}{2}\mathcal{L}(-k^2)} \tag{A.3.13}$$

which is the quantity controlling the growth of ϕ_k in the regime of small ϕ_k. The quantity $A_k := \frac{Mk^2a_4}{2L}$ controls the impact of the higher order mode coupling on the time evolution. For larger systems, the sum will include more summation terms. This effect is partially balanced out by the factor of $1/L$, suggesting a notion of "averaging" over the non-dominant modes.

A.4 Two Useful Expansions

For calculating the effective Hamiltonians, we will use the expansions

$$\frac{\left(x^2 - x^4r + x^6u\right)^2}{1 + x^2s + x^4t + x^6v} = x^4 + x^6(-2r - s) + \mathcal{O}(x^8) \tag{A.4.1}$$

and

$$\frac{\left(x^2 - rx^4\right)^2}{x^2 + tx^4} = x^2 + x^4\left(-2r - t\right) + \mathcal{O}(x^6) \tag{A.4.2}$$

to check the robustness of the discussed model, as an expansion around $x = 0$.

A.5 Meaning of the Complex Time Evolution Equation

Let $x \equiv x(t)$ and $a, b \in \mathbb{R}$. The equation

$$\partial_t x = ax + ibx \tag{A.5.1}$$

has the solution

$$x(t) = \exp\left((a + ib)t\right) x_0 e^{i\varphi_0} \tag{A.5.2}$$

where φ_0 is the complex phase of $x(t = 0)$ s.t. $x_0 \in \mathbb{R}$. If one is only interested in the magnitude of x, this is determined by

$$|x| = \exp\left(at\right) x_0 \tag{A.5.3}$$

Thereby only the real part of equation (A.5.1) determines the growth of the magnitude.

A.6 Sylvester's Criterion

Following [HJ85] Sylvester's criterion can be used to determine whether or not a hermitian (or in our case symmetric) matrix D is positive (semi)definite. It states (partially):
If D is a symmetric matrix and every principal minor of D (including $\det(D)$ itself) is non negative, then D is positive semidefinite.
We use the negated form: If D is a symmetric matrix and at least one principal minor of D (including $\det(D)$ itself) is negative, then D has at least one negative eigenvalue $\lambda < 0$.
A minor of a matrix is the determinant of a matrix that results by deleting some rows and columns. A **principal** minor is a minor in which only rows and columns with the same index are deleted.

A.7 Approximating $A_q \approx A_k$

In this thesis we abbreviated a term

$$A_k := \frac{M a_2}{2L} k^2 \tag{A.7.1}$$

where M and a_2 are non-negative[1] constants. At some point we approximated $A_k \approx A_q$. If we set $q = k + \Delta k$, we see that the relative error

$$\frac{A_q - A_k}{A_k} = \frac{2\Delta k}{k} + \mathcal{O}(\Delta k^2) \tag{A.7.2}$$

[1]The non-negativity of a_2 is bound to the requirement that $T > T_c$, which we always assume here.

scales as the ratio of $2\Delta k$, twice the deviation of q from k, to k, the reference mode.
The mode of maximal growth, i.e. that k which maximises σ_k, marks the peak of σ_q in Fig. 2.5a. Since we only look at modes with positive rate of growth, the maximum value of $2\Delta k$ is simply the width of the area of positive σ_q in Fig. 2.5a if we assume an approximately symmetric behaviour of the linear rate of growth around its maximum value. The error of $A_q \approx A_k$ therefore scales as the ratio of the position of the peak against the width of the peak.

A.8 Linear Stability Analysis

Given a differential equation

$$\dot{x} = F(x) \tag{A.8.1}$$

together with a solution x_0 with $F(x_0) = 0$, one may analyse the stability of the solution in the following way. For some small deviation δx from x_0 one has

$$\dot{x}_0 + \delta\dot{x} = F(x_0 + \delta x) \approx F(x_0) + \left.\frac{\partial F}{\partial x}\right|_{x=x_0} \delta x \tag{A.8.2}$$

Since per definition $\dot{x}_0 = F(x_0) = 0$ we know

$$\delta\dot{x} = \left.\frac{\partial F}{\partial x}\right|_{x=x_0} \delta x \Rightarrow \delta x(t) = \exp\left(\left.\frac{\partial F}{\partial x}\right|_{x=x_0} t\right) \delta x(t=0) \tag{A.8.3}$$

The deviations decrease in time if

$$\left.\frac{\partial F}{\partial x}\right|_{x=x_0} < 0 \tag{A.8.4}$$

The natural extension to multidimensional DEQs is done by replacing x with a vector $\boldsymbol{x}$ and $F(x)$ by a matrix valued function $F(\boldsymbol{x})$. To solve the DEQ for $\delta\boldsymbol{x}$ one would use the eigenvalue decomposition for F. If the eigenvectors are a basis, then every $\delta\boldsymbol{x}$ is made up of eigenvectors. The criterion for stability then extends to F having only negative eigenvalues, or $-F$ being positive definite.

A.9 Calculating the Growth of One Dominant Mode

In the case of only one mode with $\sigma_k > 0$, the DEQ we have to solve is

$$\partial_t \phi_k = \left(\sigma_k - 3A_k|\phi_k|^2\right)\phi_k \leftrightarrow \frac{\mathrm{d}x}{\mathrm{d}\tau} = \left(1 - Ax^2\right)x \tag{A.9.1}$$

where we used $A = 3A_k/\sigma_k$, $x = \phi_k$, $\tau = \sigma_k t$ and assumed w.l.o.g. that $x \in \mathbb{R}$. By using

$$\frac{1}{x - Ax^3} = \frac{1}{x} - \frac{Ax}{Ax^2 - 1} \tag{A.9.2}$$

and separation of variables we get

$$\tau + C = \int \left\{ \frac{\mathrm{d}x}{x} - \frac{1}{2}\frac{\mathrm{d}u}{u} \right\} \tag{A.9.3}$$

where we wrote $u := Ax^2 - 1$. Thereby

$$\begin{aligned} \tau + C &= \log\left(\frac{x}{\sqrt{Ax^2 - 1}}\right) \\ \Rightarrow \exp\left(2(\tau + C)\right) &= \frac{x^2}{|Ax^2 - 1|} \end{aligned} \tag{A.9.4}$$

Here we need to differentiate between $Ax^2 \lessgtr 1$. Since $Ax^2 > 1$ leads to decreasing solutions (not the behaviour we are interested in since it describes the system in an "over-excited" state) we assume $Ax^2 < 1$ and thereby get (after redefinition of the constant)

$$x = \frac{\exp(\tau)}{\sqrt{A\exp(2\tau) + \text{const.}}} \tag{A.9.5}$$

and by resubstitution

$$\phi_k(t) = \frac{\exp\left(\sigma_k t\right)}{\sqrt{\frac{3A_k}{\sigma_k}\exp\left(2\sigma_k t\right) + \text{const.}}} \tag{A.9.6}$$

From above we know that $|\phi_k^\infty|^2 = \frac{\sigma_k}{3A_k}$. We also know

$$\phi_k^2(t=0) = \frac{1}{\frac{1}{\left(\phi_k^\infty\right)^2} + \text{const.}} \tag{A.9.7}$$

and thereby

$$\text{const.} = \left(\frac{1}{\phi_k^0}\right)^2 - \left(\frac{1}{\phi_k^\infty}\right)^2 \tag{A.9.8}$$

We can therefore write

$$\boxed{\phi_k(t) = \phi_k^\infty \cdot \frac{\exp\left(\sigma_k t\right)}{\sqrt{\exp\left(2\sigma_k t\right) + \left[\frac{\phi_k^\infty}{\phi_k^0}\right]^2 - 1}}} \tag{A.9.9}$$

List of Figures

List of Tables

Bibliography

[AK07] Olaf S. Andersen and Roger E. Koeppe. "Bilayer thickness and membrane protein function: an energetic perspective." In: *Annual review of biophysics and biomolecular structure* 36 (2007), pp. 107–30. DOI: 10.1146/annurev.biophys.36.040306.132643.

[Cam+14] Felix Campelo et al. "Helfrich model of membrane bending: From Gibbs theory of liquid interfaces to membranes as thick anisotropic elastic layers". In: *Advances in Colloid and Interface Science* 208 (June 2014), pp. 25–33. DOI: 10.1016/j.cis.2014.01.018.

[Can70] P.B. Canham. "The minimum energy of bending as a possible explanation of the biconcave shape of the human red blood cell". In: *Journal of Theoretical Biology* 26.1 (Jan. 1970), pp. 61–81. DOI: 10.1016/s0022-5193(70)80032-7.

[CG09] Michael Cross and Henry Greenside. *Pattern Formation and Dynamics in Nonequilibrium Systems*. Cambridge University Press, 2009. DOI: 10.1017/CBO9780511627200.

[CH93] M. C. Cross and P. C. Hohenberg. "Pattern formation outside of equilibrium". In: *Reviews of Modern Physics* 65.3 (July 1993), pp. 851–1112. DOI: 10.1103/revmodphys.65.851.

[Des] Markus Deserno. *Fluid lipid membranes- a primer*. Lecture script from the Max-Planck-Institut für Polymerforschung. URL: https://www.cmu.edu/biolphys/deserno/pdf/membrane_theory.pdf.

[Eng05] Donald M. Engelman. "Membranes are more mosaic than fluid". In: *Nature* 438.7068 (Nov. 2005), pp. 578–580. DOI: 10.1038/nature04394.

[GGS77] C. Gebhardt, H. Gruler, and E. Sackmann. "On Domain Structure and Local Curvature in Lipid Bilayers and Biological Membranes". In: *Zeitschrift für Naturforschung C* 32.7-8 (Aug. 1977), pp. 581–596. DOI: 10.1515/znc-1977-7-817.

[Hak77] Herman Haken. *Synergetics*. Vol. 28. 9. IOP Publishing, 1977.

[Hel73] W Helfrich. "Elastic Properties of Lipid Bilayers: Theory and Possible Experiments". In: *Zeitschrift für Naturforschung C* 28.11-12 (Dec. 1973), pp. 693–703. DOI: 10.1515/znc-1973-11-1209.

[Hel85] W. Helfrich. "Effect of thermal undulations on the rigidity of fluid membranes and interfaces". In: *Journal de Physique* 46.7 (1985), pp. 1263–1268. DOI: 10.1051/jphys:019850046070126300.

[HJ85] Roger A. Horn and Charles R. Johnson. *Matrix Analysis*. Cambridge University Press, 1985. Chap. 7.2. DOI: 10.1017/CBO9780511810817.

[HR18] Takeshi Harayama and Howard Riezman. "Understanding the diversity of membrane lipid composition". In: *Nature Reviews Molecular Cell Biology* 19.5 (Feb. 2018), pp. 281–296. DOI: 10.1038/nrm.2017.138.

[Kai22] Ruth Kaiser. "Theory for Pattern Formation in Mixed Lipid Bilayers". Bachelor's Thesis. Institute of Theoretical Physics in Heidelberg, 2022.

[LA87] Stanislas Leibler and David Andelman. "Ordered and curved meso-structures in membranes and amphiphilic films". In: *Journal de physique* 48.11 (1987), pp. 2013–2018. DOI: 10.1051/jphys:0198700480110201300.

[Mai04] Philip K. Maini. "Using mathematical models to help understand biological pattern formation". In: *Comptes Rendus Biologies* 327.3 (2004), pp. 225–234. DOI: https://doi.org/10.1016/j.crvi.2003.05.006.

[MG05] Harvey T. McMahon and Jennifer L. Gallop. "Membrane curvature and mechanisms of dynamic cell membrane remodelling". In: *Nature* 438.7068 (Nov. 2005), pp. 590–596. DOI: 10.1038/nature04396.

[Nag80] J F Nagle. "Theory of the Main Lipid Bilayer Phase Transition". In: *Annual Review of Physical Chemistry* 31.1 (Oct. 1980), pp. 157–196. DOI: 10.1146/annurev.pc.31.100180.001105.

[Ple+21] Dietmar Plenz et al. "Self-Organized Criticality in the Brain". In: *Frontiers in Physics* 9 (2021). DOI: 10.3389/fphy.2021.639389.

[PS95] R. Piowsky and E. Sackmann. *Handbook of Biological Physics*. Vol. 1. Elsevier North Holland, 1995.

[Räd+95] Joachim O. Rädler et al. "Fluctuation analysis of tension-controlled undulation forces between giant vesicles and solid substrates". In: *Physical Review E* 51.5 (May 1995), pp. 4526–4536. DOI: 10.1103/physreve.51.4526.

[Ran81] R. P. Rand. "Interacting Phospholipid Bilayers: Measured Forces and Induced Structural Changes". In: *Annual Review of Biophysics and Bioengineering* 10.1 (June 1981), pp. 277–314. DOI: 10.1146/annurev.bb.10.060181.001425.

[SA95] Michael Seul and David Andelman. "Domain Shapes and Patterns: The Phenomenology of Modulated Phases". In: *Science* 267.5197 (Jan. 1995), pp. 476–483. DOI: 10.1126/science.267.5197.476.

[SJW84] M.B. Schneider, J.T. Jenkins, and W.W. Webb. "Thermal fluctuations of large quasi-spherical bimolecular phospholipid vesicles". In: *Journal de Physique* 45.9 (1984), pp. 1457–1472. DOI: 10.1051/jphys:019840045090145700.

[SR21] Cyrus R. Safinya and Joachim O. Rädler. *Handbook of Lipid Membranes*. CRC Press, July 2021. DOI: 10.1201/9780429194078.

[Tur52] A. M. Turing. "The Chemical Basis of Morphogenesis". In: *Philosophical Transactions of the Royal Society of London. Series B, Biological Sciences* 237.641 (1952), pp. 37–72. ISSN: 00804622. URL: http://www.jstor.org/stable/92463.

[Wal12] Daniel Walgraef. *Spatio-temporal pattern formation: with examples from physics, chemistry, and materials science*. Springer Science & Business Media, 2012. ISBN: 978-1-4612-7311-0.

Erklärung

Ich versichere, dass ich diese Arbeit selbstständig verfasst und keine anderen als die angegebenen Quellen und Hilfsmittel benutzt habe.

Heidelberg, den 29.4.23,